frontiers

Magnitude of the 39.8 ka Campanian Ignimbrite Eruption, Italy: a review and reassessment using an ignimbrite isopach map

Aurora Silleni[1,2*], Guido Giordano[1], Roberto Isaia[3], Michael H. Ort[2]

[1] Dipartimento di Scienze, Università di Roma Tre, Rome, Italy

[2] SES, Northern Arizona University, Flagstaff, USA, AZ

[3] Istituto Nazionale di Geofisica e Vulcanologia, Osservatorio Vesuviano, Naples, Italy

*** Correspondence:**
Corresponding Author
Aurora.Silleni@nau.edu

Keywords: Campanian Ignimbrite; Campi Flegrei; Isopach maps; Ignimbrite volumes; Pyroclastic density currents; Super-eruption.

Manuscript Length

This manuscript consists of 9335 words, 8 figures and 3 tables.

Abstract

The 39.8 ka Campanian Ignimbrite eruption is the largest caldera-forming eruption of the Campi Flegrei and had a global-scale impact on the environment and human populations. The cooling following the eruption and its widespread tephra strongly affected the paleoenvironment and the migration of hominids in Europe. Despite a large number of studies, the Campanian Ignimbrite Dense Rock Equivalent (DRE) volume estimates range from 60 to 300 km^3. Here we present a review of the previous volume evaluations and a new calculation of the volume of the ignimbrite. This estimate is constrained by the first total isopach map of the Campanian Ignimbrite PDC deposit preserved on land, developed through a method that reconstructs the paleo-topography at the time of the eruption. The method is reproducible for all strongly topographically controlled ignimbrites and allows the calculation of well-defined uncertainties in the on-land ignimbrite deposits. The preserved total extra-caldera bulk volume of the ignimbrite is estimated at 68.2 km^3 ± 6.6 km^3. The total PDC deposit volume is then corrected for erosion, ash elutriation, the intracaldera deposit volume and the volume of tephra deposited in the sea, and volumes of fallout are taken from other studies. The final total volume estimate of the eruption ranges from 177 km^3 – 265 km^3 DRE. This value corresponds to a mass of 4.6 - 6.9 x 10^{14} kg, a magnitude (M) of 7.7 – 7.8 and a volcanic explosivity index (VEI) of 7. The new detailed estimate of the Campanian Ignimbrite eruption physical parameters, for the first time constrained by the ignimbrite deposit, confirms the magnitude of this event.

1 Introduction

Pyroclastic density currents (PDCs) have large impacts on human communities and the environment; they can cause catastrophic environmental and property damage and loss of life, as well as accounting for a large proportion of deaths caused by direct volcanic activity. From 1500 to 2017 CE, 28% of volcano-induced mortality resulted from PDCs, second only to famine and epidemic disease

(Auker et al., 2013 and references therein; Brown et al., 2017). Moreover, global and regional climatic effects can result from the injection of ash and sulfur aerosols into the stratosphere during large explosive eruptions, leading to a "volcanic winter" (Rampino and Self, 1992; Stuiver et al., 1995; Thordarson and Self, 1996). The quantitative computation of the size of explosive eruptions is essential to understand their potential impact on humans, climate and ecosystems (e.g., Mason et al., 2004). Calculating the volume of large volcanic eruptions is also necessary to define their size (e.g., Newhall and Self, 1982; Pyle, 2000, 2015; Crosweller et al., 2012) and to model the climate effects of these natural phenomena that occurred in the past.

Large (volcanic explosivity index ≥ 4; e.g., Crosweller et al., 2012) caldera-forming eruptions produce both fall deposits and ignimbrites (Parfitt and Wilson, 2008), and typically the largest proportion of volcanic material is transported in PDCs and emplaced as ignimbrites (e.g., the Oruanui eruption; Wilson, 1991; the Otowi Member of the Bandelier Tuff; Cook et al., 2016). The tephra fall deposits are analyzed through field and statistical techniques to make isopach maps directly from thickness data (e.g., Walker and Croasdale, 1970; Walker, 1973; Rhoades et al., 2002; Burden et al., 2013; Engwell et al., 2015; Yang and Bursik, 2016; Cutler et al., 2020), from which numerical models can be used to calculate total volumes (Bonadonna et al., 1998; Bonadonna and Phillips, 2003; Bonadonna and Houghton, 2005; Folch et al., 2010; Costa et al., 2012; Folch, 2012). The resulting tephra volumes appear to be better constrained than ignimbrite volumes, where a clear "reference" method does not exist and uncertainties on such computations are significant (Mason et al., 2004).

Calculation of the volume of ignimbrites has been the subject of numerous studies (Walker, 1983; Aldiss and Ghazali, 1984; Henry and Price, 1984; Morgan et al., 1984; Ratté et al., 1984; Sparks et al., 1985; Scott et al., 1996; Wilson, 2001; Pérez et al., 2006; Giordano et al., 2010; Folkes et al., 2011; Best et al., 2013a, 2013b; Cook et al., 2016; Pacheco-Hoyos et al., 2018; Takarada and Hoshizumi, 2020), but it remains difficult to evaluate due to the irregularity of the ignimbrite surface, the variable thickness (controlled by the paleotopography; e.g., Yokoyama, 1974: Wilson 1991; Broxton and Reneau, 1996: Daag and van Westen, 1996), the effect of erosion (e.g., Yokoyama, 1985), the presence of overlying deposits, and the variable density of the deposits. The eruptive volume, and as a consequence the ignimbrite volume, is essential for computation of the magnitude (M; Mason et al., 2004) and volcanic explosivity index (VEI; Newhall and Self, 1982) of an eruption. The calculation of the volume of ignimbrites, which form the main part of eruptions with M > 5, remains one of the outstanding issues in volcanology (e.g., the collapse caldera database (CCDB) project, Geyer and Martí, 2008; the LAMEVE project, Crosweller et al., 2012).

The lack of a standardized accurate method for the calculation of ignimbrite volumes makes most of the existing figures for large-volume ignimbrites poorly constrained and, in many cases, unreproducible, resulting in a wide range of estimated volumes of the same ignimbrite (e.g., Cerro Galán, Folkes et al., 2011; Campanian Ignimbite, Scarpati et al., 2014). The case study for this work is the Campanian Ignimbrite (CI; Barberi et al., 1978; Fisher et al., 1993; De Vivo et al., 2001; Fedele et al., 2008), associated with the most powerful caldera-forming eruption from the Campi Flegrei caldera (CF) (Fig. 1A) (Rosi and Sbrana, 1987; Perrotta et al., 2006; Scarpati et al., 2013). It is one of the largest late Quaternary explosive events and has been considered as an example of a super-eruption (Sparks et al., 2005). The 39.8 ka CI tephra (Plinian and co-ignimbrite products; Giaccio et al., 2017) represents the most widespread volcanic deposit and one of the most important temporal/stratigraphic markers for the Early Upper Paleolithic of Western Eurasia (Fedele et al., 2003; Pyle et al., 2006; Giaccio et al., 2008). The eruption may have affected human residents in different ways: by destroying the animal and human populations, by altering the species composition

and growth rhythm and by changing the availability of water (Fedele et al., 2002, 2003, 2007; Lowe et al., 2012). The abrupt volcanic cooling following the eruption produced a regional drop of 6°C to 9°C in Eastern Europe and Northern Asia (Black et al., 2015). The cooling could have influenced the migration of the populations and have affected the daily life for Neanderthals and modern humans during the Middle to Upper Paleolithic transition (Fedele et al., 2002, 2003; Black et al., 2015; Marti et al., 2016).

In this work, we present a review of all articles that calculated the CI volume. Despite the large number of studies, the estimates of total Dense Rock Equivalent (DRE) volume of the CI eruption range from 60 to 300 km^3 (Thunell et al., 1979; Cornell et al., 1983; Rosi et al., 1983, 1999; Fisher et al., 1993; Civetta et al., 1997; Fedele et al., 2003; Perrotta and Scarpati, 2003; Rolandi et al., 2003; Giaccio, 2006; Marianelli et al., 2006; Pyle et al., 2006; Pappalardo et al., 2008; Costa et al., 2012; Scarpati et al., 2014; Marti et al., 2016). Furthermore, none of these studies provides a solid method to determine the ignimbrite volume in the Apennine Mountains. The volume of dispersed tephra (both Plinian and co-ignimbrite) was better defined due to the many measurements across the vast region blanketed by the CI ash and a recent improvement of computational methods (Costa et al., 2012; Marti et al., 2016), as well as by the simpler nature of its mantling deposition. In contrast, the volume of the ignimbrite deposits has never been calculated by accurate direct measurements, but only by approximate thicknesses (Thunell et al., 1979; Fisher et al., 1993; Civetta et al., 1997; Giaccio, 2006). Here, we assess the ignimbrite volume using precise thickness measurements and reporting those on an isopach map. We demonstrate a rigorous method to create a complete isopach map of the CI, with a similar approach to that normally applied to tephra-fall deposits (e.g., Engwell et al., 2015) and it can be easily used on other ignimbrites in the world. The map is based on the mapping of the preserved ignimbrite deposits, without the fall deposits, and reconstruction of the paleotopography, especially mountainous areas. This allows us to provide an accurate estimate of the volume of the extra-caldera deposits of the CI pyroclastic density current preserved on land based on a verifiable method of calculation and with the relative uncertainties. Using this as a base, we correct for erosion, elutriation, intracaldera volume and underwater deposits to calculate the, up to date, most reliable total bulk and DRE volumes for this ignimbrite. We then estimate the co-ignimbrite volume and add the fallout volume from previous studies to calculate the total erupted volume for the eruption. The obtained eruptive volume significantly reduces the total uncertainty of the total volume calculation and should be used to better design and constrain the eruptive dynamics. Such data, well constrained and evaluated, from many volcanoes could help determine the frequency of eruptions of a given magnitude around the world.

2. Volcanological background

Volcanic activity in the Campi Flegrei began prior to 80 ka (Pappalardo et al., 1999; Scarpati et al., 2013) and caldera collapses occurred during the eruptions of the CI, the ~15 ka Neapolitan Yellow Tuff (NYT) eruptions (Orsi et al., 1996; Perrotta et al., 2006; Acocella, 2008; Vitale and Isaia, 2014) and the M 6.6 event Masseria del Monte Tuff correlated to the Y-3 marine tephra (Albert et al., 2019). Post-NYT activity in the caldera is well described by Di Vito et al. (1999), Isaia et al. (2009) and Smith et al. (2011).

The CI eruption emplaced both pyroclastic fall and PDC deposits in a complex sequence currently exposed in proximal, sporadic medial, distal and ultra-distal outcrops (Fig. 1) (Barberi et al., 1978; Rosi et al., 1988, 1996, 1999; Fisher et al., 1993; Perrotta and Scarpati, 1994, 2003; Orsi et al., 1996; De Vivo et al., 2001; Cappelletti et al., 2003; Perrotta et al., 2006; Fedele et al., 2008; Engwell et al., 2014; Scarpati et al., 2015a, 2015b; Sparice, 2015; Scarpati and Perrotta, 2016; Smith et al., 2016).

The first phase of the eruption generated Plinian columns up to 44 km high (Rosi et al., 1999; Marti et al., 2016), producing a widespread fall deposit dispersed by winds to the east (Rosi et al., 1999; Perrotta and Scarpati, 2003; Marti et al., 2016; Scarpati and Perrotta, 2016). A pyroclastic density current then spread over an area of 7,000 km^2 and surmounted ridges more than 1,000 m high (Barberi et al., 1978; Fisher et al., 1993). This stage caused the caldera collapse and the accumulation of lithic breccia deposits (Breccia Museo) in scattered outcrops along the caldera rim (Perrotta and Scarpati, 1994; Melluso et al., 1995; Rosi et al., 1996; Fedele et al., 2008). In distal outcrops, most of the CI is represented by a massive, gray ignimbrite (Barberi et al., 1978; Fisher et al., 1993; Scarpati and Perrotta, 2012; Scarpati et al., 2015a). Beyond about 80 km from the vent, deposits are made up of coarse to fine ash containing both co-Plinian and co-ignimbrite tephra (Thunell et al., 1979; Sparks and Huang, 1980; Engwell et al., 2014; Smith et al., 2016). The tephra marker related to this eruption is essential to correlate volcanological and archaeological sites in the Mediterranean area and Eastern Europe. Tephra-based correlations of human sites were used to date the Middle to Upper Paleolithic transition (Giaccio et al., 2008; 2017; Lowe et al., 2012).

The complex stratigraphy of this eruption differs between proximal and distal outcrops. Moreover, it is difficult to study the lateral correlations due to the absence of outcrops in medial areas (except for the Lago di Patria outcrop, Table 2 in Data Repository), because all quarry-pits have been refilled. The limited drill core data shows little evidence of lateral unit change. In our study, we refer to the stratigraphic units proposed by Fedele et al. (2008) (proximal area) and Cappelletti et al. (2003) (distal areas) (Online Supplementary Material). The first flow unit is the unconsolidated stratified ash flow (USAF) both in proximal and distal stratigraphy, which is followed by the main units of Piperno and Breccia Museo inside the caldera and the welded gray ignimbrite (WGI) and lithified yellow tuff (LYT) in medial and distal outcrops.

3. Estimating eruption volume

Most studies of eruptive volume focus their attention on the Plinian fallout and the ignimbrite phases of volcanic eruptions, but the total volume calculation is a complex result of many different components. The total volume erupted during a caldera-forming eruption, like the CI, is composed of the mass ejected during the phases that produced Plinian columns (V_{Pcol}), and pyroclastic density currents (V_{pdc}) (1):

$$\boldsymbol{V = V_{Pcol} + V_{pdc}} \quad (1)$$

Both V_{Pcol} and V_{pdc} refer to the primary deposits (respectively the Plinian fallout V_{Pfall}, the proximal pumice lapilli deposit, and the ignimbrite V_{ign}) and their associated co-Plinian fall ($V_{coPfall}$) and co-ignimbrite ash fall (V_{coign}), respectively. Indeed, fine ash suspended in the atmosphere can be co-Plinian rather than co-ignimbrite (Fierstein and Hildreth, 1992). In this work, the co-Plinian ash is defined as the fine-grained Plinian ash, decoupled from the coarser fallout and subject to atmospheric turbulence (Fierstein and Hildreth, 1992). The co-ignimbrite ash is considered to be the buoyant material that rises from the PDC through the entrainment, heating and expansion of ambient air (Woods and Wohletz, 1991), and may represent the counterpart to the crystal-enriched ignimbrite (Sparks and Walker, 1977). Consequently (2):

$$\boldsymbol{V = (V_{Pfall} + V_{coPfall}) + (V_{ign} + V_{coign})} \quad (2)$$

The erosion and re-deposition can subsequently modify these components before measurement of the thicknesses occurs. In the following sections, we discuss different methods used in the past to

estimate the CI eruption volume. The CI is not a unique example and those methods have been applied on many eruptions (e.g., Pyle, 1989).

3.1 *The previous estimates of the CI eruptive volume*

A synopsis of the previously determined estimates of the total volume is provided in Table 1.

Due to the difficulty to distinguish the contribution of the co-Plinian fall and the co-ignimbrite ash fall in ultra-distal locations, some authors simply refer to the widespread Y-5 ash layer, which comprises both (Table 1) (Thunell et al., 1979; Cornell et al., 1983; Rolandi et al., 2003; Costa et al., 2012). Other previous studies distinguished the co-Plinian and co-ignimbrite contribution (Sparks and Huang, 1980; Perrotta and Scarpati, 2003; Engwell et al., 2014; Marti et al., 2016; Smith et al., 2016), but only some of them calculated the relative volumes (Perrotta and Scarpati, 2003; Marti et al., 2016).

3.1.1 *From direct measurements*

The first volume estimate of the ignimbrite was presented by Thunell et al. (1979). Based on a geometrical method that considers a covered area of over 6,000 km^2 with a thickness up to 100 m and assuming radial flow of the PDC, they estimated the DRE volume was at least 30-40 km^3. The DRE volume of the Y-5 ash layer within the 1-cm isopach contour was also estimated at 30-40 km^3 (65 km^3 bulk). Their total DRE volume was 60-80 km^3 for the eruption.

Cornell et al. (1983) calculated the ash-fall layer volume of Y-5 from an isopach map derived by different cores drilled in the Mediterranean Sea (73 km^3 bulk). They then included the ignimbrite DRE volume proposed by Thunell et al. (1979) in their overall eruption volume estimate. On the other hand, the bulk volume of the original pyroclastic current deposit was estimated by Fisher et al. (1993) to be about 500 km^3 by circumscribing a circle of deposits with a radius of 100 km, 100 m thick at the center that thinned to zero at the perimeter of the circle, with no consideration of topography.

Rosi et al. (1999) calculated the bulk volume of the Plinian fallout as 15 km^3 based on the method proposed by Pyle (1989); in the CI eruption, the focus of the elliptical isopach distribution corresponds to a central vent located in the Campi Flegrei caldera center (town of Pozzuoli). The authors used thickness values from distal outcrops, up to 64 km from the vent. The same technique was used by Perrotta and Scarpati (2003), who estimated a bulk volume of about 4 km^3, the different value of this work being the result of a different isopach model compared to the one used by Rosi et al. (1999). In the same paper Perrotta and Scarpati (2003) attempted, for the first time, to discriminate between the volumes of the co-Plinian and co-ignimbrite components. The coarse ash of ultra-distal deposits was interpreted as the co-Plinian phase, while the fine ash represents the co-ignimbrite component. The authors evaluated the thicknesses of the two parts and estimated 16 km^3 bulk of co-Plinian ash and 100 km^3 bulk of co-ignimbrite ash.

These analyses were then improved by Pyle et al. (2006), who used ultra-distal thickness values all over Eastern Europe. The authors estimated the minimum bulk volume of the CI fallout at 74 km^3 or 31 km^3 DRE (using magma density of 2,400 kg/m^3 and 1,000 kg/m^3 bulk deposit density) using Pyle's (1989) general observation that many fallout deposits show exponential decay of thickness. Pyle et al. (2006) compared these results with a second approach based on the rate of thinning of the distal ash sheets (based on Pyle, 1989, 1990): given that the thickest ash layer in marine cores is in the order of 10–20 cm, it is most likely that the total bulk ash volume associated with the eruption

was in the range 74-120 km^3 (31–50 km^3 DRE) (Pyle et al., 2006). Scarpati and Perrotta (2016) subdivided the fallout into five layers (A to E) on the basis of grain size, component variations and graded bedding. The volumes for each layer were calculated using the exponential fitting method of Pyle (1989), obtaining a primary fallout of about 5 km^3 (~1 km^3 DRE, using a magma density of 2,400 kg/m^3 proposed by Rosi et al., 1999) and a co-Plinian ash of about 15 km^3 (~7 km^3 DRE, using the same magma density as the primary fallout).

A first attempt to collate all the volume estimates was made by Fedele et al. (2003), who considered the sum of the conservative estimates reported in literature (the sum of the fallout, the PDC deposits and the Y-5 ash layer volumes; Thunell et al., 1979; Civetta et al., 1997; Rosi et al., 1999). The total DRE volume they proposed is 200 km^3, using a bulk deposit density of around 1,250 kg/m^3. Rolandi et al. (2003) proposed the same volume (200 km^3 DRE, 320 km^3 bulk), consisting of 180 km^3 bulk of PDC (150 km^3 in proximal area and 30 km^3 in distal area, obtained by the analysis of seismic data, drill-holes, and considering the areal extent of the deposits) and 140 km^3 bulk of the distal ash (80 km^3 in the Mediterranean Sea and 60 km^3 as ultra-distal tephra, using an isopach map).

A similar value was proposed by Giaccio (2006), 215 km^3 DRE (385 km^3 bulk), who calculated the volume of the PDC using a complex truncated cone, with a concave surface and variable heights: 70 m up to 10 km from the center, 50 m up to 20 km, 20 m up to 45 km and 0 m up to 100 km. At the same time, he proposed a revised isopach map for the fallout deposits, resulting in a volume estimate of 10 km^3 (3 km^3 DRE). Moreover, combining all available data on the distal tephra of CI from the literature (Cornell et al., 1983; Melekestsev et al., 1984; Paterne et al., 1986; McCoy and Cornell, 1990; Cini Castagnoli et al., 1995; Seymour and Christanis, 1995; Narcisi and Vezzoli, 1999; Ton-That et al., 2001; Upton et al., 2002; Seymour et al., 2004), Giaccio (2006) calculated the volume of the distal fraction as 180 km^3 (86 km^3 DRE) and thus estimated a bulk volume of 575 km^3 (300 km^3 DRE). The DRE volumes were calculated using a bulk density, ranging between 1,400 and 2,500 kg/m^3 for the ignimbrite, 1,200 kg/m^3 for the distal ash and 800 kg/m^3 for the fallout pumices.

3.1.2 *From petrological data and numerical modeling*

Civetta et al. (1997) is one of the first works that subdivided the volume of the CI eruption based on the pumice composition. The authors divided the magma into three different types: a most evolved one that consists of Plinian fallout and some ignimbrite up to 50 km from the vent (a volume of 25 km^3 DRE), a magma with intermediate composition that includes some of the ignimbrite out to its farthest extent (100 km^3 DRE), and a least-evolved magma that includes much of the ignimbrite in the Campanian Plain (20 km^3 DRE). All the volume calculations were made by circumscribing circles with a radius similar to the maximum distance reached from the vent by that magma type and a thickness that goes from the maximum thickness of ignimbrite of that given composition at the caldera center to zero at the perimeter of the circle.

Marianelli at al. (2006) proposed different crystallization depths suggested by the results of CI melt inclusion studies and then estimated the volume of the eruption directly from a magma chamber model, attributing 20 km^3 DRE to the fallout deposits, and 130 km^3 DRE to the ignimbrite. The method was not explained with more details in the article (Marianelli et al., 2006). Pappalardo et al. (2008) used petrological data to constrain the pre-eruptive magma storage dynamics analyzing the different magma compositions for each eruptive phase. In agreement with Civetta et al. (1997), Pappalardo et al. (2008) proposed a total volume of 200 km^3 DRE based on a major and trace element modeling (20 km^3 for the fallout and 180 km^3 for the ignimbrite). The authors used the total porosity of each analyzed sample, which varies between 0.36 and 0.93, with an average of 0.58.

Costa et al. (2012) proposed a new tephra volume estimate based on the fit of an advection – diffusion tephra dispersion model to thickness data (more than 100 ultra-distal locations). They obtained a bulk volume of the tephra of 250-300 km^3 (104-125 km^3 DRE, the model assumes an average bulk deposit density of 1,000 kg/m^3) and a total volume of the eruption of 430-680 km^3 (180-280 km^3 DRE).

Scarpati et al. (2014) estimated the PDC volume applying equation (3) (see below) assuming a co-ignimbrite volume (V_{coign}) of 100 km^3 obtained by Perrotta and Scarpati (2003) and a mean vitric loss of 0.65. The method is based on the enrichment factor of Walker (1972, 1980) and the vitric loss of the ignimbrite proposed by Sparks and Walker (1977). The ignimbrite volume (V_{ign}) (3) is equal to:

$$V_{ign} = \frac{V_{coign}}{vitric\ loss} - V_{coign} \quad (3)$$

This method is strongly influenced by the mean value of vitric loss used, which is normally estimated from sporadic point measurements. The bulk volume of the PDC deposits thus estimated is 54 km^3 (25 km^3 DRE, using a density of 2,600 kg/m^3). In the same study, the authors proposed a review of the previous volume estimations (Scarpati et al., 2014).

The most recent work on the fallout volume was presented by Marti et al. (2016). The authors recognized two distinct plume phases: the Plinian (V_{Pcoi}) and the co-ignimbrite fall. They applied a computational inversion method that explicitly accounts for the two phases and for gravitational spreading of the umbrella cloud. Dividing the modeling in two different eruptive phases provides the best estimate, as they are two different spreading and source phenomena. The Plinian fallout bulk volume thus calculated is 54 km^3 (22.6 km^3 DRE, using a magma density of 2,500 kg/m^3) and the co-ignimbrite bulk volume as 153.9 km^3 (61.6 km^3 DRE), for a total bulk volume of 207.9 km^3 (84.2 km^3 DRE).

To summarize, the range in volumes is wide (an order of magnitude, $54 - 500\ km^3$, in bulk volume) due to the different methods used, which is a problem in view of the importance of such figures in calculating the impact on climate and the environment. While the computational methods for the fallout deposits have improved significantly in the past ten years and the related figures for the CI fallout phase appear strong and solidly based on field data (Costa et al., 2012; Marti et al., 2016), the volume figures for the CI ignimbrite are still poorly constrained by field data and lack well-assessed (epistemic) uncertainties. The ignimbrite volume also affects the estimate of the volume of elutriated co-ignimbrite ash, which is the dominant fallout phase across Europe and the main fraction of ash injected into the stratosphere by the eruption (e.g., Costa et al., 2018).

4. Methods

4.1 Investigated CI eruptive unit

In order to reduce this wide range in volume estimates, we focus on constraining the volume of the ignimbrite deposits of the CI, as this is the most poorly constrained at present. We use volumes calculated by Perrotta and Scarpati (2003) and Marti et al. (2016) for the initial pyroclastic Plinian fall phase and the co-ignimbrite fallout to estimate the total erupted volume. Our CI isopach map is based on previous published data, new fieldwork and the assessment of the paleo-topographic control exerted on the deposits thickness distribution.

4.2 Density measurements

More than 40 samples from different outcrops scattered around the Campanian Plain were analyzed to determine their density. Samples were cut in cylinders (with radius between 0.9 and 2 cm and height between 0.8 and 5.7 cm) or cubes (sides from 0.8 to 2.5 cm) and analyzed using a Micromeritics AccuPyc II 1340 helium pycnometer. The instrument provides a standard deviation for each measurement that was used to evaluate the density errors. The resulting density was used to interpret total and open porosity. Open porosity was estimated with geometric (V_g) and matrix volume (V_{mx}): $100*(V_g-V_{mx})/V_g$, while closed porosity was determined using the DRE of the WGI and Piperno powder, which was obtained by the pycnometer. The total porosity (φ_t) was calculated directly by summing closed and open porosity. The density is used to determine the DRE volume.

4.3 Database and fieldwork

Published data regarding CI thickness and outcrop locations were collected from 42 papers (presented in Data Repository, Table 1). The data were inserted in a GIS Open-Source QGIS 3.4 (https://www.qgis.org/it/site/) database including 238 localized outcrops. The database includes the location name, the lithological description, the geographic coordinates, the elevation a.s.l., the thickness of the flow units (specifying whether total or minimum outcrop thickness), the maximum lithic dimensions and the degree of welding. Where both base and top of the CI are exposed, the thickness is classified as total and elsewhere it is considered a minimum thickness. The database reports raw thickness data and adjustments due to erosion are explained later on.

This database has been augmented by our field data acquired in 97 locations (presented in Data Repository, Table 2), both in proximal and distal areas (Fig. 1A). At these new field sites, information on total or minimum thickness, to verify the local stratigraphy, and the relation of the ignimbrite to topography was collected.

4.4 Defining the CI PDC deposit extent

The 0-m isopach is an outer limit beyond which the CI is not present, and it delimits the current areal distribution of the ignimbrite outcrops. The isopach was reconstructed through a first phase of revision of the geological maps already existing at the scale 1:50,000 or 1:100,000 (Servizio Geologico d'Italia, 1963, 1965, 1966, 1967, 1971a, 1971b, 1975; ISPRA, 2009, 2010, 2011a, 2011b, 2011c, 2011d, 2014a, 2014b, 2016, 2018). The contact was traced between the CI and older units and extrapolated where CI does not crop out. In this circumstance, the ignimbrite is generally covered by younger deposits, so it is necessary to assess if the CI was emplaced in these locations. To do this, a statistical and morphological analysis of the slope of the top of the CI was applied and a comparison between the topography and the average slope of the CI top was carried out. Where the slope angle is comparable, the area was included in the 0-m isopach, even if CI does not crop out. The underlying basement (mostly Meso-Cenozoic calcareous or flysch rocks) has generally higher slope angles than the CI (for example the Apennine flanks), so the CI produces a morphologically distinct slope. The isopach was traced to leave out high-slope areas and no primary CI deposition was interpreted. The slope analysis was performed on a slope map developed using a 10-m resolution Digital Elevation Model (DEM) (Tarquini et al., 2007; Tarquini et al., 2012; Tarquini and Nannipieri, 2017). The statistical and morphological analysis of the upper surface of the CI used 48,804 points distributed throughout the areal extent of the deposits (both in proximal and distal areas).

4.5 The isopachs

To determine the isopach locations, two different methods were used, one in the proximal area to medial (from the caldera to the base of the Apennine Mountains, including the Campanian Plain) and one in the distal area. The almost complete lack of outcrops in the Campanian Plain and the valley-ponded depositional style in the ridge-valley topography of the Apennine Mountains (Rosi et al., 1983, 1996; Perrotta et al., 2010; Langella et al., 2013; Scarpati et al., 2014, 2015a; Sparice, 2015; Fedele et al., 2016) make these different approaches necessary.

In the proximal-medial area, data from the literature (Ortolani and Aprile, 1985; Scandone et al., 1991; Bellucci, 1994; Rolandi et al., 2003; Milia and Torrente, 2007; Torrente et al., 2010; ISPRA, 2011d), consisting of more than 300 thickness values of CI from boreholes, outcrops and geological sections were used to fit isopachs on the map (Online Supplementary Material). In the distal area, the isopach locations were based upon our field observations and a reconstruction of the pre-CI topography (Fig. 2), which was a separate analysis based on series of ~ 150 profiles in the Apennine Mountains, drawn to outline the trend of the valleys (Fig. 2B). The coastline of the Mediterranean Sea at the time of the CI emplacement (39.8 ka) was lower than today. Based upon limited sea-level correlation work in the Mediterranean basin (Lambeck and Bard, 2000; Antonioli et al., 2004; Antonioli, 2012), we assumed a sea level between 75 m and 87 m below the present level.

Topographic cross-sections were traced orthogonally to the center of the valley and to the contour lines, including the flanks of the reliefs and the 0-m isopach. The slopes of the valley above the CI 0-m isopach were extended and gradually deepened toward the valley center in order to reconstruct the paleo-valley with an inclination of the sides similar to the current slope, always taking into consideration the geological and morphological features (Fig. 2B), and assuming that the Meso-Cenozoic mountain slopes have not significantly changed since 40 ka. The base elevation of the paleo-valleys is constrained by field data where the CI base has been measured.

These reconstructed valleys culminate generally in a V shape, not considering the CI that filled them, with the bottom elevation, for each profile, representing the paleo-valley floor. All these elevations represent the ancient pattern of the valley bottom, for this reason, they were modified if they were inconsistent with the progressive downslope decrease in elevation towards the sea.

Finally, the neo-incision of rivers in the profiles was "filled in", so as to remove the linear erosion of the last 39.8 kyr, drawing a line that reproduces the original ignimbrite deposit before that the erosion occurred (Fig. 2B). The CI thickness is calculated from these modified profiles, and it is from the top of the deposit obtained by the profiles into the paleo-valley slope. However, the thickness is always constrained by field data of the CI thickness and by the geological maps. These thickness values are then reported on the isopach map.

All the isopachs were traced in accordance with fieldwork, looking both to the base CI elevation and the CI thickness, the geology of Meso-Cenozoic valley sides and, finally, the present-day drainage network compared to the paleo-valleys during the eruption (Fig. 2). Where these data were not consistent, an adjustment in some profiles was necessary. In some cases, a correction was made for an over-thickening in the valleys caused by an over-deepening of the extended valley sides, not consistent with field observations. In these cases, the thickness was modified in coherence with fieldwork.

We use, as a starting point for the volume estimate, the ignimbrite deposits volume obtained from the detailed isopach map. This information is lacking in previous estimates of the CI volume. We refer to

all PDC units of the CI as the CI, without distinguishing them; in the medial and distal outcrops, the CI is mainly composed of WGI.

5. Results

5.1 The isopach map

The morphological analysis shows that 64% (31,057) of the points have slopes lower than 5°. Moreover, 88% of the points have slopes lower than 15° and 99% have a surface slope lower than 55° (Fig. 3). The CI slope values are consistent with field observations during this work and in agreement with the observation on the slope of the top surface of the valley-ponded Taupo Ignimbrite, which is around 8° (Wilson and Walker, 1985).

Based on these results, the 0-m isopach was traced to enclose all the mapped CI and areas that probably have the CI below the recent sedimentary cover, they have a slope less than 15° and they are in contact with mapped CI outcrop. The 15° slope is consistent with the results, and it allows the inclusion of all the possible CI extent. With this approach, some CI-containing valleys are isolated from the main CI deposits (Fig. 4). The isolated valleys contain some CI outcrops, but they are confined by high slope or basement deposits nearby, and they are separated from the main ignimbrite by post-emplacement erosion. The total area enclosed by the 0-m isopach of the CI is 3,216 km^2 (Fig. 4). To understand also the total area of the region inundated by the PDC, and avoid underestimation, a shape was drawn comprising all the maximum areal extension of the isopach 0-m. The enveloped area is 6,095 km^2 (Online Supplementary Material), similar to the 6,000 km^2 estimate of Thunell et al. (1979).

The isopach map traced in the proximal area does not include the intracaldera deposits. The maximum thickness in proximal areas is 80 m (Fig. 5), mainly based on outcrops near the caldera rim; the CI thins gradually away from the caldera margin. The detailed isopach maps show the area of thickening or thinning in the Campanian Plain and in the Apennines (Fig. 6). The isopach for the distal reaches has a maximum thickness of 50 m in the Valle dei Maddaloni (Fig. 6C). In distal areas, a series of confined valleys show local thickening.

5.2 Density of the CI deposits

The bulk density (ρ) of the WGI samples ranges from 745 ± 15 kg/m^3 to 1,330 ± 3 kg/m^3, with an average of 980 ± 11 kg/m^3 (see section 4.2 to methods on how the errors were calculated). Error-free measures for all samples follow a Gaussian distribution with a standard deviation of the Gaussian probability density function of 127 kg/m^3. The bulk density of the Piperno unit ranges from 1,275 ± 8 kg/m^3 to 1,302 ± 2 kg/m^3, with an average of 1,287 ± 4 kg/m^3 (presented in Data Repository, Table 3). The total WGI porosity ranges from 49 ± 5% to 71 ± 5% and the average is 61.6 ± 5%. The average for the Piperno unit it is 50 ± 1%. The total porosity matches with the range used by Pappalardo et al. (2008). The ρ DRE is 2,607 ± 31 kg/m^3, which is in agreement with the magma density used by Scarpati et al. (2014). The DRE volume is determined multiplying the bulk volume by (100- φ_t)/100.

5.3 Deposits volume calculation

Data were plotted in a semi-logarithmic plot (Fig. 7) in which thickness (T) and area (A) follow the relation: $T=T_{max} \cdot \exp(-k_1 A)$ (Wilson, 1991). T_{max} of the CI from this relation is 71.3 m (the measured value in the field is 80 m), k_1 is equal to 10^{-3} m^{-2} and r^2 is 0.929. These values were obtained plotting thickness and area with the same unit (m).

Following this equation, the volume is the definite integral of the function, where the area of each isopach was calculated directly from the QGIS software. Table 2 displays the values of the area and the volume for each isopach extrapolated by the function (Fig. 7). Summing all the isopach volumes, the total volume of the preserved extra-caldera CI deposits on land is 68.2 ± 6.6 km^3 (26.8 ± 2.6 km^3 DRE). The sources of error and the uncertainties were calculated separately for the proximal and medial area and for the distal one; their calculation is explained in the Online Supplementary Material. The CI volume was compared to other ignimbrites, whose bulk volumes span three orders of magnitude: the Lund Ignimbrite (4,400 km^3; Best et al., 2013a), the Greens Canyon Tuff (GCT, 600 km^3; Best et al., 2013a), the Petroglyph Cliff (40 km^3; Best et al., 2013a), the Oruanui Ignimbrite (300 km^3; Wilson, 1991) and the Pozzolane Rosse ignimbrite (RED, 35 km^3; Giordano et al., 2010; Giordano and Doronzo, 2017) (Fig. 7).

To understand the extra-caldera volume subdivision in proximal and distal areas, the isopach map is divided into two parts, one comprising all the Campanian Plain, and the other from the first Apennine ridges to the final runout (Fig. 5). The resulting extra-caldera volumes are 48.6 ± 1.7 km^3 in the proximal area (~70%) and 19.6 ± 4.9 km^3 in the distal area (~30%).

6. Discussion

The linear relations between log10 thickness and area presented in Fig. 7 show all the ignimbrites have r^2 values above 0.9. k_1 varies between 10^{-4} m^{-2} and 10^{-3} m^{-2} for each ignimbrite, but it seems that bigger ignimbrites (Lund and Oruanui ignimbrites) have lower k_1 values. The concavity of this curve gives information on the aspect ratio of the deposits: concave-upward curves (i.e. convex) refer to low-aspect-ratio deposits while concave-downward curves apply to high-aspect-ratio ignimbrites (Wilson, 1991). The CI shows an intermediate aspect ratio, with the first part of the curve upward and the second downward, which reflects the field evidence, noticed during the fieldwork, of both low and high aspect ratio behavior of the CI. GCT and RED show a similar change in concavity. The RED shows similar features to the CI in the field: both ignimbrites encountered topographic barriers perpendicular to the flow, such that the RED climbed topographic barriers as high as 400 m (Giordano et al., 2010) while the CI overtopped 1,000-m barriers. Such interaction has an important role in the flow dynamics (e.g., Bursik and Woods, 2000; Andrews and Manga, 2011) and it is associated with a decrease in carrying capacity and an increase of the sedimentation rate (Giordano, 1998). The change of the curve concavity could directly show the sedimentation rate fluctuations.

6.1 Extracaldera volume

The data from this work were compared with Ruberti et al. (2020), who proposed contour maps of the lower and the upper surfaces of the CI for the northwestern sector of the proximal-medial area, based on 1,000 lithostratigraphic logs from boreholes. The extrapolated thicknesses from their maps were compared with the isopach map of this work by drawing a new proximal isopach map based on their contour maps. The volume calculated from this new isopach map is 46.5 km^3, 2.1 km^3 less than the volume we estimated. This difference is included in the 6.6 km^3 of the total volume error and uncertainties here presented. The data proposed by Ruberti et al. (2020) were not inserted in the isopach map reported in this work to avoid error propagation due to data coming from contour maps rather than deposit thickness measurements. However, a greater thickness in the Volturno Plain compared to this work could be considered, as proposed by Ruberti et al. (2020).

The error and uncertainties associated with our volume estimate of the terrestrial CI ignimbrite deposits (68.2 ± 6.6 km^3) are less than 10% (Online Supplementary Material), a good precision

464 considering that many published estimates of eruption volume may be barely more precise than one
465 order of magnitude (Mason et al., 2004). The accuracy of the applied method is also due to the
466 development of the 0-m isopach areal extent. Cutler et al. (2020) demonstrated that the inclusion of
467 zero values improved the modeling and the volume calculations for tephra layers of Mount St Helens.
468 Moreover, the complexity of the isopach shapes, instead of simplified oblate shapes, allows better
469 consideration of raw thickness data and lessens inaccurate volume estimates (Engwell et al., 2015).
470 This method can now be applied to ignimbrite deposits, with a good parallelism between flow and
471 fall volume calculations.

472 The volume we presented above is not the total volume of the CI PDC deposits, but the preserved
473 extra-caldera ignimbrite volume and several corrections must be applied to this value (Mason et al.,
474 2004; Folkes et al., 2011). Each factor has relative uncertainties, but here we constrain them to a
475 well-defined preserved extra-caldera volume and we analyze each minimum and maximum volume.
476 A significant amount of pyroclastic material was deposited in the sea and within the caldera,
477 significant erosion has occurred in the last 39.8 kyrs, and a large amount of co-ignimbrite ash
478 elutriated or rose into the air as a column.

479 The reconstructed isopachs do not consider the linear erosion due to river incision of the CI so the
480 possible areal erosion must be calculated. The linear erosion is related to the selective erosion due to
481 rivers, while the areal erosion comprises all the regional processes that occurred in the area. The
482 deposits of WGI show a mainly valley-ponded deposit pattern; in many areas where the ignimbrite
483 was deposited in narrow valleys (for instance near Roccamonfina), the only unit that mantles the
484 topography is USAF, while the upper surface of WGI is mainly horizontal (Fig. 3) (Sparice, 2015).
485 This suggests that USAF is a facies emplaced over a wider area than WGI, comprising also
486 topographic highs with mantling and veneer features, but was then subjected to significant areal
487 erosion (Wilson, 1991). The thickness of USAF is mainly between 10 cm and 1 m; in rare cases, it
488 can reach 3 m (Fedele et al., 2016). A median thickness of 1 m is assumed as eroded material for all
489 the enveloped area (6,095 km^2, projected area) not covered by valley-pond facies, as a reference for
490 the areal erosion. To calculate the erosion, we used the real surface of the enveloped area. The real
491 surface is the actual surface of an area, not its projection, and it considers also the mountain slopes.
492 From the DEM, the real surface was computed at 9,575 km^2. The volume associated with the areal
493 erosion, on the real surface, is 9.6 km^3 (V_e) (3.7 km^3 DRE, using the average density of WGI). This is
494 a correction based on field observations (USAF mantling the topography) and an average calculation
495 (the thickness and the area) could vary if the eroded thickness, or involved area, are substantially
496 different from those assumed here.

497 The CF caldera is located near and below the current sea-level but, about 40 ka, the coastline was
498 farther to the southwest corresponding to a level between 75 and 87 m below its present position
499 (Lambeck and Bard, 2000; Antonioli et al., 2004; Antonioli, 2012) (Fig. 8). Based on the distribution
500 on land of the ignimbrite, the assumed radial spreading (Thunell et al., 1979; Fisher et al., 1993; Ort
501 et al., 2003), and the position of the CF caldera relative to the coastline (Fig. 8), a roughly equal
502 amount of material should be present both on land and offshore. The bathymetry offshore shows
503 depressions and valleys south of the caldera that could be areas of ignimbrite deposit accumulation
504 (Fig. 8). Flow deposits of Kos and Krakatau demonstrate that PDCs can travel considerable distances
505 above sea water (Carey et al., 1996; Allen and Cas, 2001; Dufek and Bergantz, 2007) and it is known
506 the Campanian PDC flowed over the water of the Bay of Naples to deposit on the Sorrento Peninsula
507 (~ 35 km from Pozzuoli Bay to Sorrento) (Fisher et al., 1993).

The occurrence of turbidity currents in the Mediterranean basin coeval with the eruption was confirmed by analyses of the core CT85-5 in the Tyrrhenian Sea (40°19'02''N, 11°15'42''E), more than 200 km west of the CF caldera (Cini Castagnoli et al., 1995; Giaccio, 2006; Giaccio et al., 2006; Hajdas et al., 2011). The 45-cm-thick CI tephra recognized within the core was used as an important time marker. The nearby CT85-6 confirmed the presence of the CI tephra, but it was less studied as its record is shorter and the CI tephra is not reported fully (Hajdas et al., 2011). The CI layer contains shallow water gastropods and internal lamination, which indicate that at least 10 cm of the section are from turbiditic origin (Cini Castagnoli et al., 1995; Giaccio, 2006; Hajdas et al., 2011). These volcaniclastic currents related to the CI eruption are reported throughout the Tyrrhenian basin (McCoy and Cornell, 1990; Giaccio, 2006) and interpreted as the results of large syn-eruptive transport of the CI material as the PDCs entered the water. The turbidity currents can be reasonably considered as primary products of the eruption (Giaccio, 2006). Milia et al. (2020) report the presence of a debris flow related to the CI eruption in the CET2 core (39°55.23′ N, 14°07.56′ E) and an erosive surface in the nearby CET1 core (39°54.69' N, 14°06.65' E), both located in the lower bathyal zone offshore of the Campania margin. These authors recognized the CI's impact in the area and the possible generation of a tsunami related to the eruption.

For these reasons, a large amount of underwater material is realistic and, because of the nearly equal radial area covered by sea versus on land, is considered equal to the on-land material, so each is considered to have a volume of 68.2 $km^3 \pm 6.6$ km^3 (V_m). However, the total volume that entered the water during and after the eruption was equal to the preserved volume on land plus the eroded volume (68.2 km^3 + 9.6 km^3).

6.2 Intracaldera volume

Wells were drilled since the 1940s to understand the deep geothermal system in Campi Flegrei, reaching depths of 1,600-3,000 m below ground surface (Rosi and Sbrana, 1987). A strong hydrothermal alteration was recognized, with four main zones marked by distinctive mineral assemblages. These wells reached the CI units, but the extensive hydrothermal alteration prevented its identification. Due to the high uncertainties of correlating CI deposits inside the caldera, the isopach map was traced without the intracaldera area and the intracaldera volume was not estimated in this work.

More recently, a 506-m borehole was drilled west of Naples, penetrating both the NYT and CI (Mormone et al., 2015; De Natale et al., 2016). The hydrothermal alteration in the proximity of CI (around 439 and 501 m) was recognized and made the correlation with the deposits extremely difficult. However, through lithological, mineralogical and $^{40}Ar/^{39}Ar$ dating the authors recognized around 250 m of intracaldera CI (De Natale et al., 2016). This thickness value was previously observed through geological and geophysical features (Torrente et al., 2010). The ignimbrite volume inside the caldera was then estimated at less than 16 km^3, using a caldera dimension of 64 km^2 (De Natale et al., 2016).

There are some uncertainties due to the caldera's true shape. Vitale and Isaia (2014) proposed a 12-km-wide polygonal caldera, which corresponds to an area of 144 km^2, while De Natale et al. (2016) suggested a minimum area of 64 km^2. Considering an average thickness of 250 m of intracaldera deposits (De Natale et al., 2016), and an area varying from 64 to 144 km^2, the intracaldera volume (V_{intr}) ranges between 16 km^3 and 43.2 km^3 (7.9-21.4 km^3 DRE, using the proximal unit density of the Piperno).

6.3 Distal tephra volume

The CI tephra is an important correlation tool and time marker for Quaternary stratigraphy in different basins and archaeological sites in Western Eurasia. The tephra layer is visible in numerous sedimentary records, including marine (Keller et al., 1978; Paterne et al., 1986, 1999; Ton-That et al., 2001), terrestrial sequences (Veres et al., 2013), cave-entrance environments (Fedele et al., 2003; Giaccio et al., 2008), lacustrine records (Narcisi, 1996) and archaeological sites (e.g., Badino et al., in press and references therein). The occurrence of the CI tephra in archaeological sites helps to address the human bio-cultural evolution at the Middle-Upper Paleolithic transition in Italy (Castelcivita, Serino and Grotta del Cavallo sites; Gambassini, 1997; Giaccio et al., 2008 and references therein; Lowe et al., 2012; Wood et al., 2012; Zanchetta et al., 2018), in Montenegro (Crvena Stijena; Morley and Woodward, 2011; Mihajlovic and Whallon, 2017), in Greece (Douka et al., 2014; Zanchetta et al., 2018) and in Russia (Kostenki; Giaccio et al., 2008 and references therein). In very distal sites, it can be found as a cryptotephra not visible to the naked eye, but clearly useful as an absolute and relative chronological and stratigraphic marker (Lowe et al., 2012).

Defining the distribution of the ultra-distal deposits is a difficult task due to the limitation of the field data available and to the thinning of the ash layers. Underestimation of the deposit volume can be derived by simple extrapolation from proximal, medial and distal data to the ultra-distal region. The case of the CI is complicated by the presence of both co-Plinian fallout ash and co-ignimbrite fallout ash, both transported far from the vent through to Eastern Europe and Russia (Thunell et al., 1979; Cornell et al., 1983; Narcisi and Vezzoli, 1999; Fedele et al., 2003; Giaccio et al., 2006; Pyle et al., 2006; Engwell et al., 2014; Smith et al., 2016).

Nevertheless, the ultra-distal tephra volume is necessary to define the total CI eruptive volume. Sparks and Huang (1980) recognized the bimodal grain-size of the ultra-distal deposits of the CI, interpreting the coarse lower unit as formed during the Plinian phase, and the finer upper unit as the co-ignimbrite phase. These features were also observed by Wulf et al. (2004) at Monticchio Lake. Sparks and Huang (1980) estimated that the fine layer represents, on average, 65% of the tephra volume and increases in proportion away from the vent, from 20% at 450 km to 95% of the deposit at 1,660 km from the vent. However, an absolute volume for each phase was not defined. The decreasing of Plinian material with distance from the source was also observed by Engwell et al. (2014), who used the grain-size data to investigate the dispersal of the co-Plinian and the co-ignimbrite phases. The authors calculated that 40 ± 5% of the volume of tephra within 850 km of the vent is related to the Plinian phase (as a consequence, around 60% relates to the co-ignimbrite phase, in agreement with Sparks and Huang, 1980). Furthermore, they recognized the difficulty in quantifying the absolute volume of the two phases, due to the complexity of separating the two layers in more distal deposits.

Smith et al. (2016) used the CI tephra glass composition to map the dispersal of the Plinian and co-ignimbrite components over the dispersal region. Based on the glass composition, the authors recognized that the PDC component is dominant in the ultra-distal deposits, and the PDC produced the most voluminous deposits of the eruption.

Summarizing, a significant part of the pyroclastic current was elutriated or rose into the atmosphere as a co-ignimbrite cloud during the eruption and dispersed to the east (Thunell et al., 1979; Cornell et al., 1983; Perrotta and Scarpati, 2003; Pyle et al., 2006; Engwell et al., 2014; Scarpati and Perrotta, 2016). The co-ignimbrite phase was a substantial part of the total volume; but it remains difficult to define the associated absolute volume rather than as a percentage of the tephra layer.

6.4 The volume, mass and magnitude of the CI eruption

The bulk ignimbrite volume (V_{ign}) (4 and 5) without the co-ignimbrite phase can be estimated as follows:

$$V_{ignmin} = V_{pr} + V_m + V_{intr} + 2V_e = 61.6 + 61.6 + 16 + 9.6 + 9.6 = 158.4\ km^3 \quad (4)$$

and

$$V_{ignmax} = V_{pr} + V_m + V_{intr} + 2V_e = 74.8 + 74.8 + 43.2 + 9.6 + 9.6 = 212.0\ km^3 \quad (5)$$

The total bulk PDC volume obtained using (4) and (5) is 158.4 – 212.0 km^3 (Table 3). The co-ignimbrite volume (V_{coign}) is estimated using the formula (6) based on the crystal concentration method proposed by Scarpati et al. (2014) (3):

$$V_{coign} = \frac{Vitric\ loss * V_{ign}}{1 - Vitric\ loss} = \frac{0.65 * V_{ign}}{1 - 0.65} = 294.2 - 393.7\ km^3 \quad (6)$$

The co-ignimbrite volume, using a vitric loss of 0.65, ranges between 294.2 km^3 and 393.7 km^3 (115.8 km^3 – 155.0 km^3 DRE), producing the highest of all previous estimates. However, V_{coign} could change significantly based upon the value of vitric loss used. Walker (1972) proposed a vitric loss of 0.55 for a WGI outcrop at Altavilla, near Benevento. Using this datum, the co-ignimbrite bulk volume decreases to between 193.6 km^3 and 259.1 km^3. In this work, we use 0.65, as proposed by Scarpati et al. (2014), which is an average of more samples located in several distal sites all over the CI distribution, and from different units but it is not far from 0.55 proposed by Walker (1972). Because the calculation of the V_{coign} is beyond the purpose of this work, an alternative is to use the minimum and maximum co-ignimbrite volume reported in the literature, which are between 72 km^3 and 153.9 km^3 bulk (31 km^3 – 61.6 km^3 DRE; respectively from Pyle et al., 2006 and Marti et al., 2016), but it is worth considering that this may be a significant underestimate.

The total volume of the material erupted during the PDC phase of the CI eruption ranges between 452.6 km^3 and 605.7 km^3 (175.8 km^3 – 242.6 km^3 DRE) (Table 3). This estimate is based on the preserved deposits of the CI. Among the previous estimates presented in the literature, the closest to our PDC volume are those proposed by Giaccio (2006) and Pappalardo et al. (2008).

Using the previously published fallout volume (the minimum and the maximum proposed; Perrotta and Scarpati, 2003; Marti et al., 2016), in combination with our PDC volume, gives a total eruptive volume of all eruptive phases of 456.6 km^3 to 659.7 km^3 (177.5 km^3 – 265.2 km^3 DRE) (Table 3). However, any of the previous estimates for the fallout volume could be used in our total volume estimate. These values are similar to some previously proposed total volumes (Cornell et al., 1983; Fedele et al., 2003; Giaccio, 2006; Pyle et al., 2006; Pappalardo et al., 2008; Costa et al., 2012), but they are constrained, for the first time, by direct thickness measurements of the ignimbrite deposit.

The mass associated with this volume, using our density estimate is (7):

$$mass_{min} = 177.5\ km^3 * 2,608\ kg/m^3 = 4.63 * 10^{14} kg \quad (7)$$

And (8):

$$mass_{max} = 265.2\ km^3 * 2,608\ kg/m^3 = 6.92 * 10^{14} kg \quad (8)$$

and the magnitude (M) (9) (Mason et al., 2004):

$$M = log10(mass) - 7 = 7.7 - 7.8 \quad (9)$$

This value is consistent with a VEI 7 and a M = 7.7 – 7.8 and confirms this eruption as the largest Quaternary event in Europe, as proposed previously in the LAMEVE project (M = 7.7; Crosweller et al., 2012).

7. Conclusions

The CI eruption is the largest eruptive event of the CF caldera and a fundamental chronological marker in all Central and Eastern Europe. Here we presented a review of previous estimates in the scientific literature and proposed a new method to trace ignimbrite isopachs based on the extrapolation of the paleo-topography. It works well in valley-ponded ignimbrites such as the CI, and allows the calculation of well-defined uncertainties in the on-land total volume. Before the present study, no complete isopach map of the ignimbrite was available, due to the high irregularities of the deposits. A new isopach map of the extracaldera sub-aerial CI pyroclastic flow deposits yields a volume of 68.2 $km^3 \pm 6.6$ km^3, based directly on deposit thickness values. The greater part of this volume is in the proximal area (48.6 ± 1.7 km^3, ~70%) while only around the 30% of the volume is in the distal region within the Apennine Mountains (19.6 ± 4.9 km^3). The method, similar to those used for tephra deposits, can be used on other ignimbrites, to produce more accurate volume estimates.

Evidence suggests that the same amount of material should be both on land and offshore (assuming radial spreading of the flow). The generated submarine currents could have deposited a large amount of volcaniclastic deposits in all the submarine canyons in the Gulf of Naples and in the Tyrrhenian Sea and possibly had a strong impact on the underwater dynamics of that area. Combining separate estimates of the marine volume, the volume removed by erosion, the intracaldera volume, and the co-ignimbrite ash volume yields a total volume of 453 km^3 to 606 km^3 (176 km^3 – 243 km^3 DRE) for the PDC deposits. These values are in agreement with Giaccio (2006) and Pappalardo et al. (2008), although it is the first time that they are calculated by direct measurements with constrained error estimates. This work deals with the importance of constraining eruptive volume with field data, presenting a rigorous method to develop ignimbrite isopachs that avoids the inaccuracy of approximate techniques and defines step-by-step techniques for isopach construction and the error corrections. This is the first attempt to estimate ignimbrite volume in a comparable way to tephra fallout volume and by direct thickness data. The development of isopach maps for ignimbrite deposits, especially in complex topographic areas, is the most accurate instrument to calculate ignimbrite volumes, and is better than approximate techniques using average thicknesses or conical shapes. A rigorous definition of the 0-m isopach, the isopachs and each correction factor is necessary to avoid inexact volumes. Field data remain an essential tool to constrain primary properties of PDCs.

The total (including Plinian fallout) final volume estimate is 457 km^3 – 660 km^3 (177 km^3 – 265 km^3 DRE). This volume corresponds to a mass of 4.6 - 6.9 x 10^{14} kg, to a magnitude of 7.7 – 7.8 and to a VEI 7. This was a high-impact event that likely had significant effects on the climate and populations of the Paleolithic European region and is a proof that the Campi Flegrei volcano was able to generate a devastating eruption of this dimension.

2 Article types

Original Research

673 # 3 Manuscript Formatting

674 ## 3.1 Figure legends

675

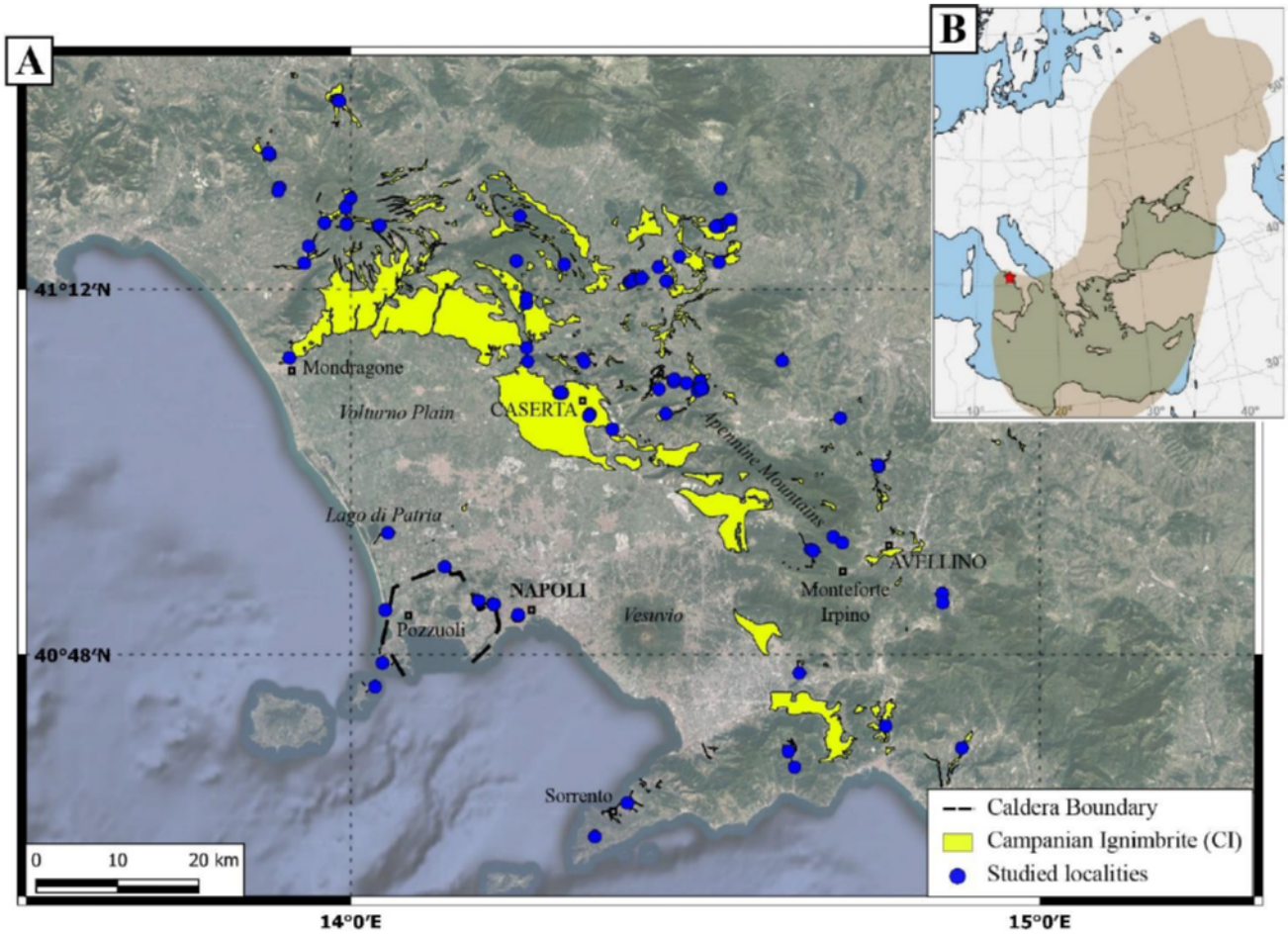

676

677 ***Figure 1.*** *The Campanian Ignimbrite distribution.* ***(A)*** *The Campanian Ignimbrite distribution in the*
678 *Campanian region (the base map is from Google Satellite), defined merging fieldwork and*
679 *geological maps (Servizio Geologico d'Italia, 1963, 1966, 1967, 1971a, 1971b, 1975; ISPRA, 2009,*
680 *2010, 2011a, 2011b, 2011c, 2011d, 2014a, 2014b, 2016, 2018). Blue dots indicate the location of the*
681 *studied exposures (coordinates are reported in the data repository).* ***(B)*** *Dispersal area of the CI*
682 *tephra from the Campi Flegrei caldera (red star), modified from Giaccio et al. (2017). The maps*
683 *were generated using the QGIS Open-Source 3.4 (https://www.qgis.org/it/site/).*

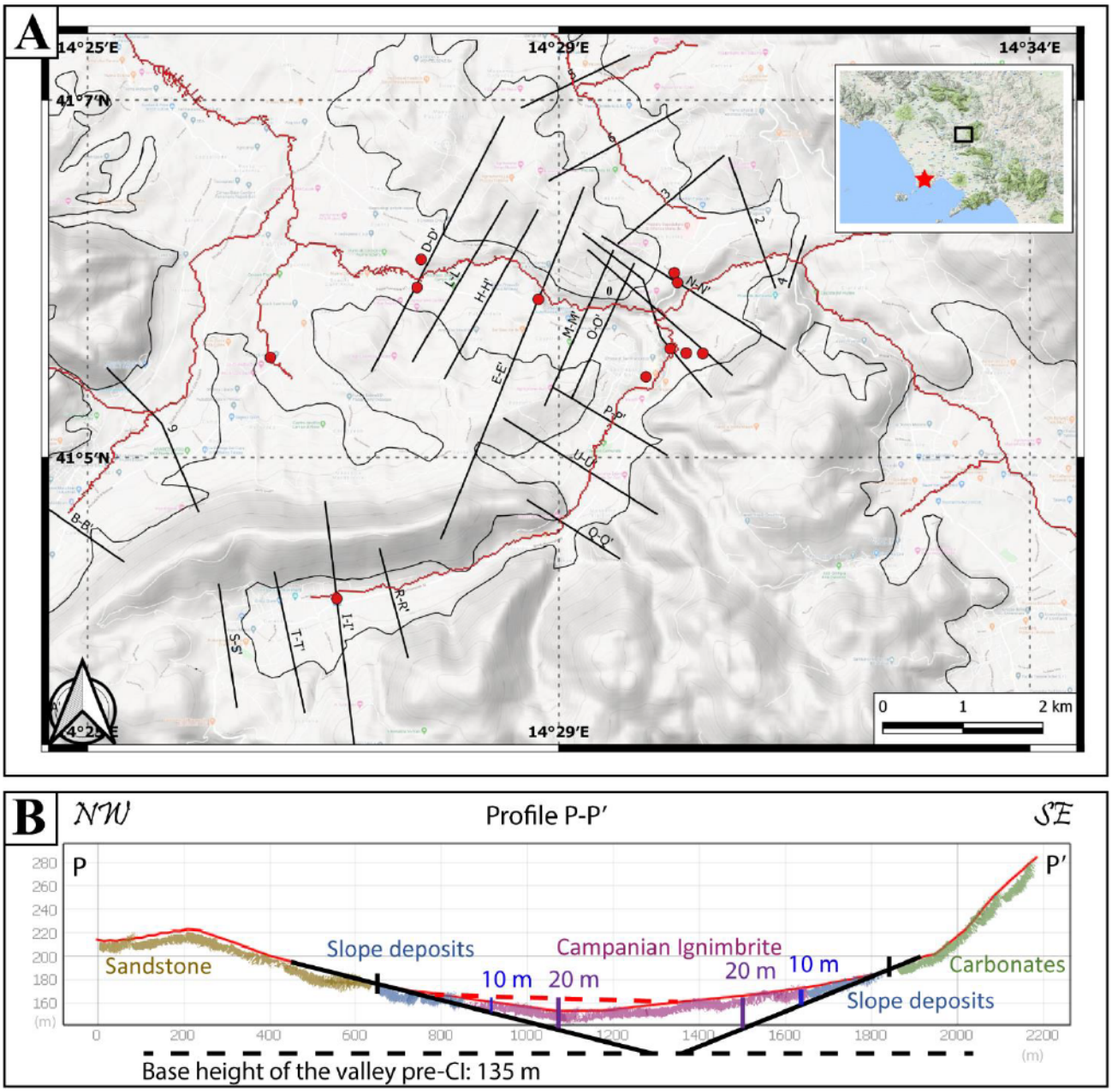

Figure 2. *The topographic reconstruction in the Sant'Agata dei Goti area (reported in the right corner, the red star is the vent).* ***(A)*** *A series of profiles traced to study the paleo-valley; the red dots are the studied outcrops where the CI is exposed. The red lines represent the river network developed through the QGIS software, while the black line is the 0-m isopach.* ***(B)*** *Reconstruction of the paleo-valley in profile P-P', the base elevation is constrained to the CI base observed by fieldwork and to the current slope of the valley. The resulting thickness is coherent with fieldwork, so where thicknesses are too high, they were not considered and the isopachs were traced up to a realistic thickness. The numbers represent the thickness of the CI in meters. The different colors represent different types of deposits, while the dashed red line, is the linear erosion that occurred in 39 kyrs.*

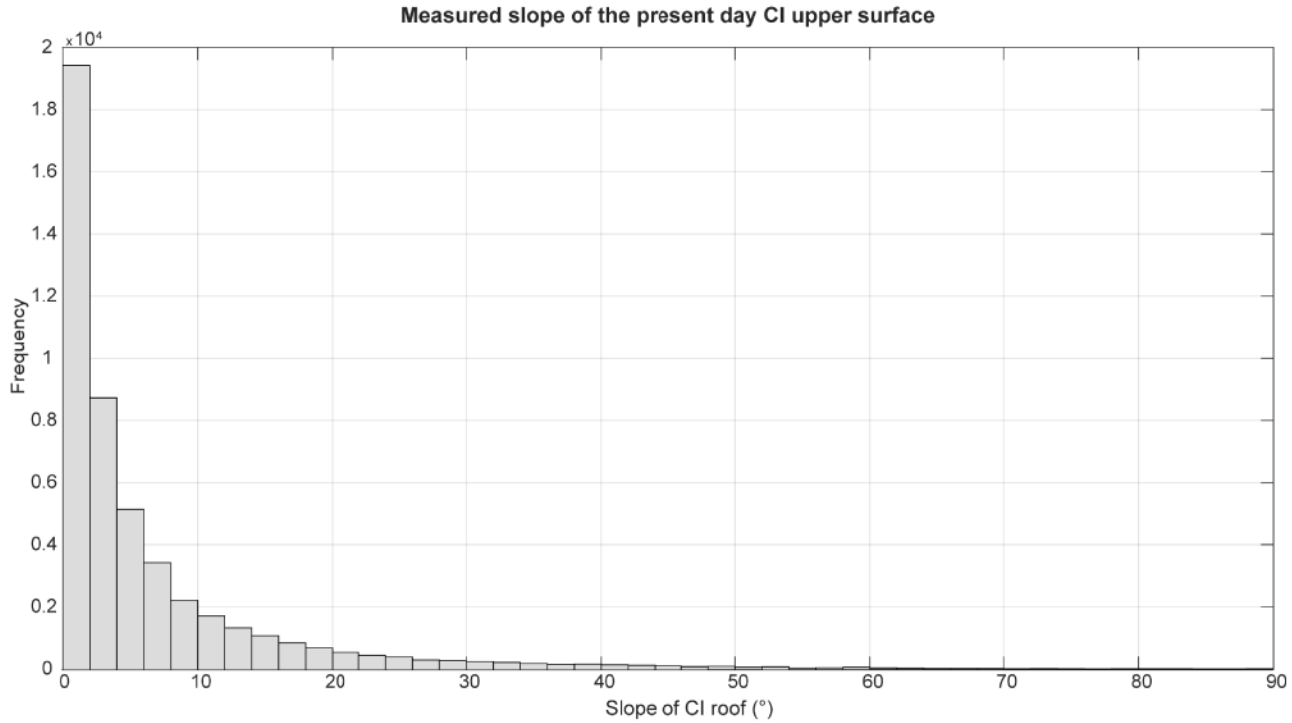

694

695 ***Figure 3.*** *Frequency of the slope of the upper surface of the CI. At least 80% of the exposed CI upper*
696 *surface slopes less than 10°. The areas with slope greater than 35° are related to river incisions and*
697 *CI escarpments.*

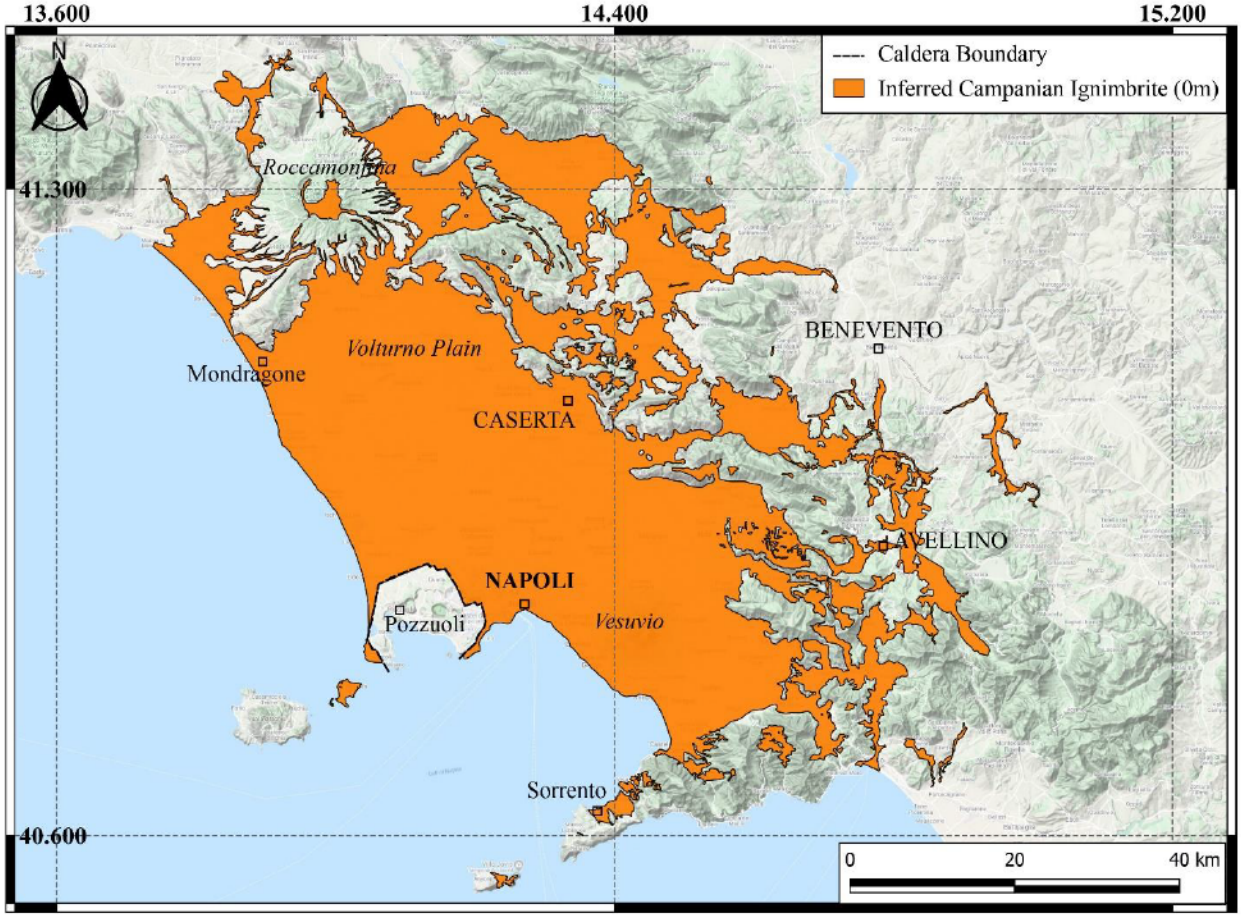

Figure 4. *Reconstruction of the areal extent of the ignimbrite deposits, enclosed within the 0-m isopach is shown in orange. The total area covered by the preserved deposits of CI is 3,216 km^2, the envelopment with a shape is equal to 6,095 km^2 (Online Supplementary Material). The isolated areas from the source are due to the erosion of veneer facies.*

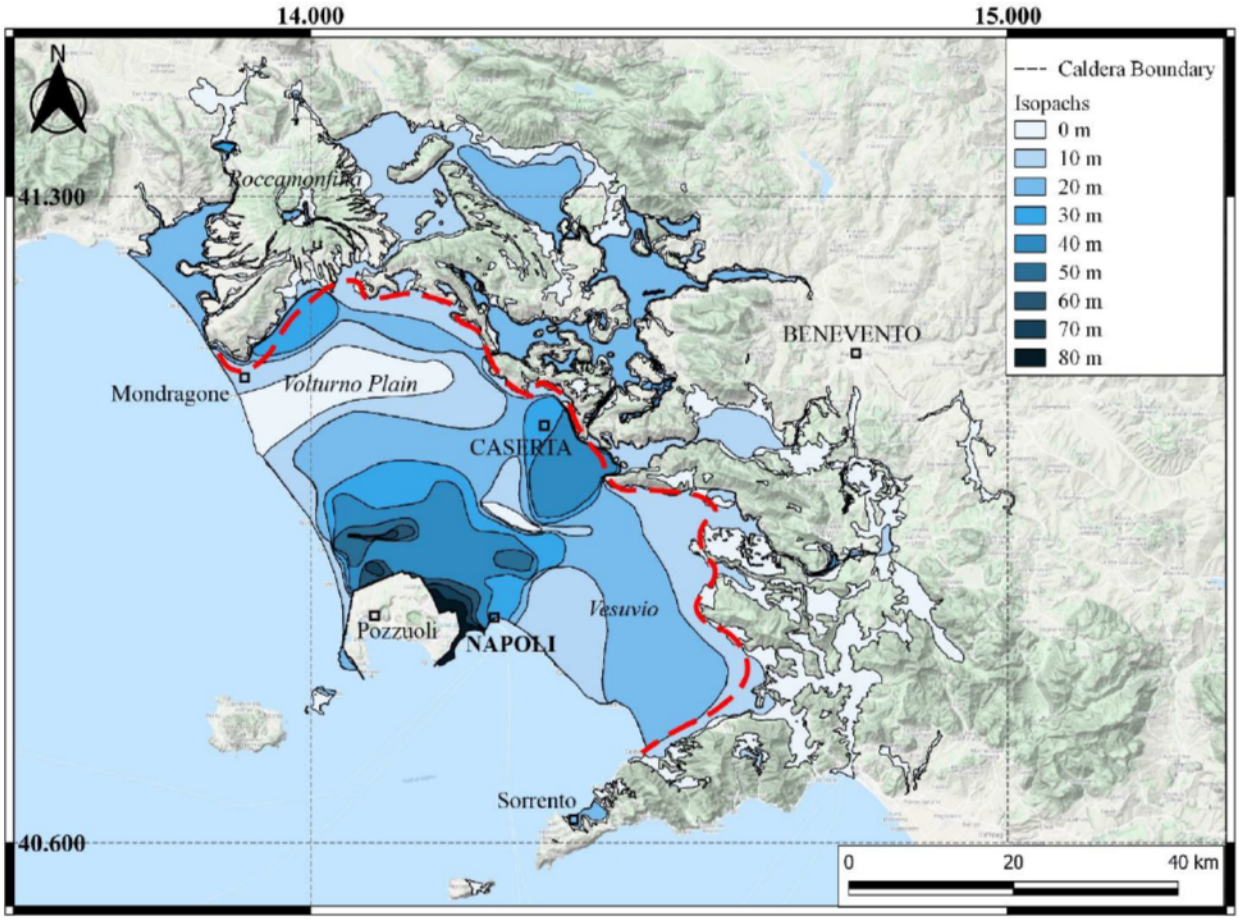

Figure 5. *Isopach map of the preserved extra-caldera deposits of the Campanian Ignimbrite. This map refers only to the ignimbrite deposits; it excludes the Plinian fallout and the co-ignimbrite ash. The different colors for each isopach are reported in the map key. The red dashed line divides the proximal and the distal area.*

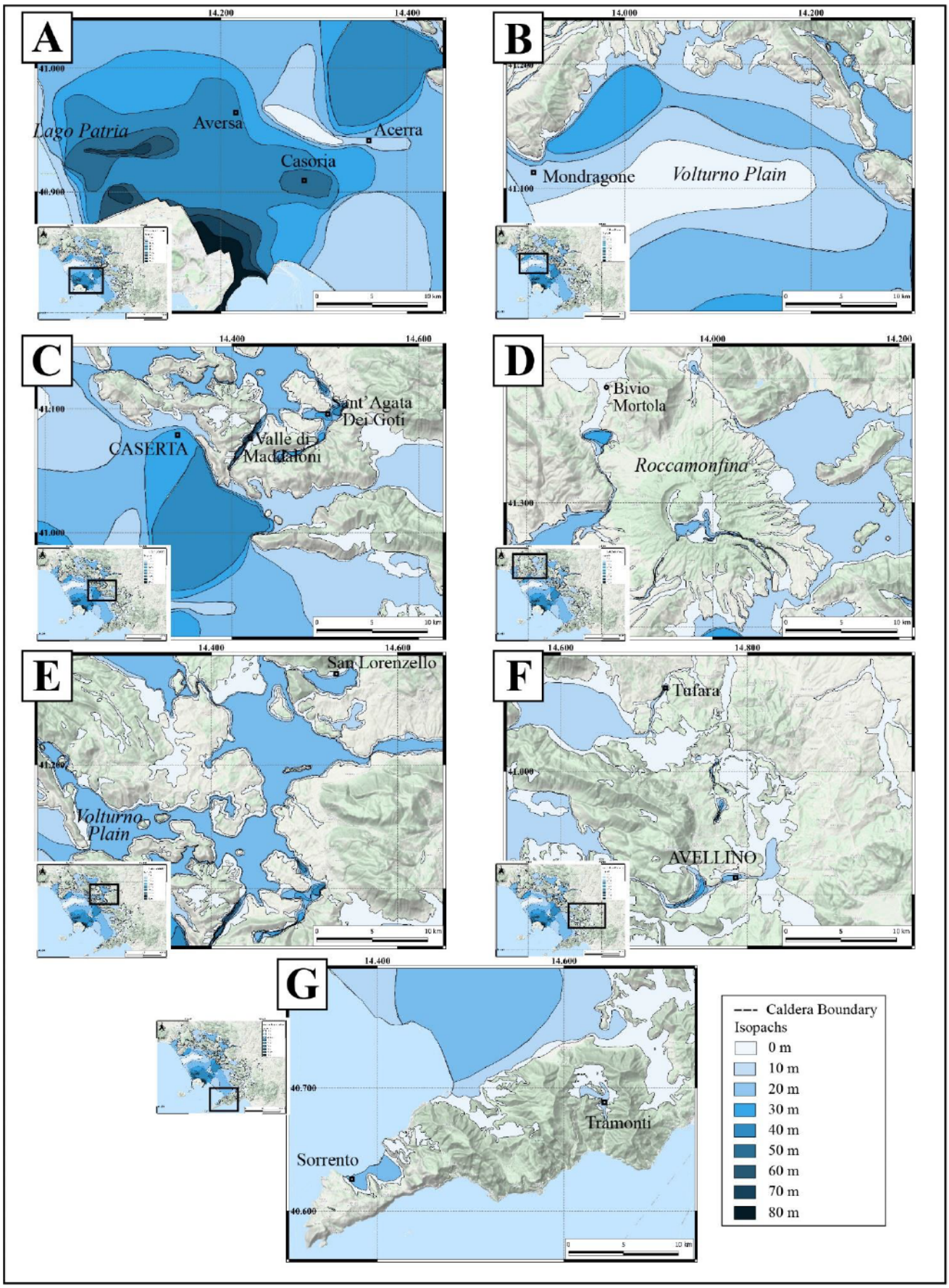

Figure 6. *Detailed isopach maps of selected areas of the Campanian Ignimbrite (excludes fallout): (A) north of the caldera, between Lago Patria and Acerra; (B) northern part of the Campanian Plain; (C) Apennine ridges east of the Campi Flegrei caldera and the Valley of Maddaloni; (D) Roccamonfina and Mortola, in the north of the studied area; (E) Volturno plain and San Lorenzello area, northeast of the caldera; (F) distal area of Avellino, southeast of the caldera; (G) Sorrento peninsula, in the southern part of the studied area. See section 4.5 to detailed methods on how the isopachs were traced.*

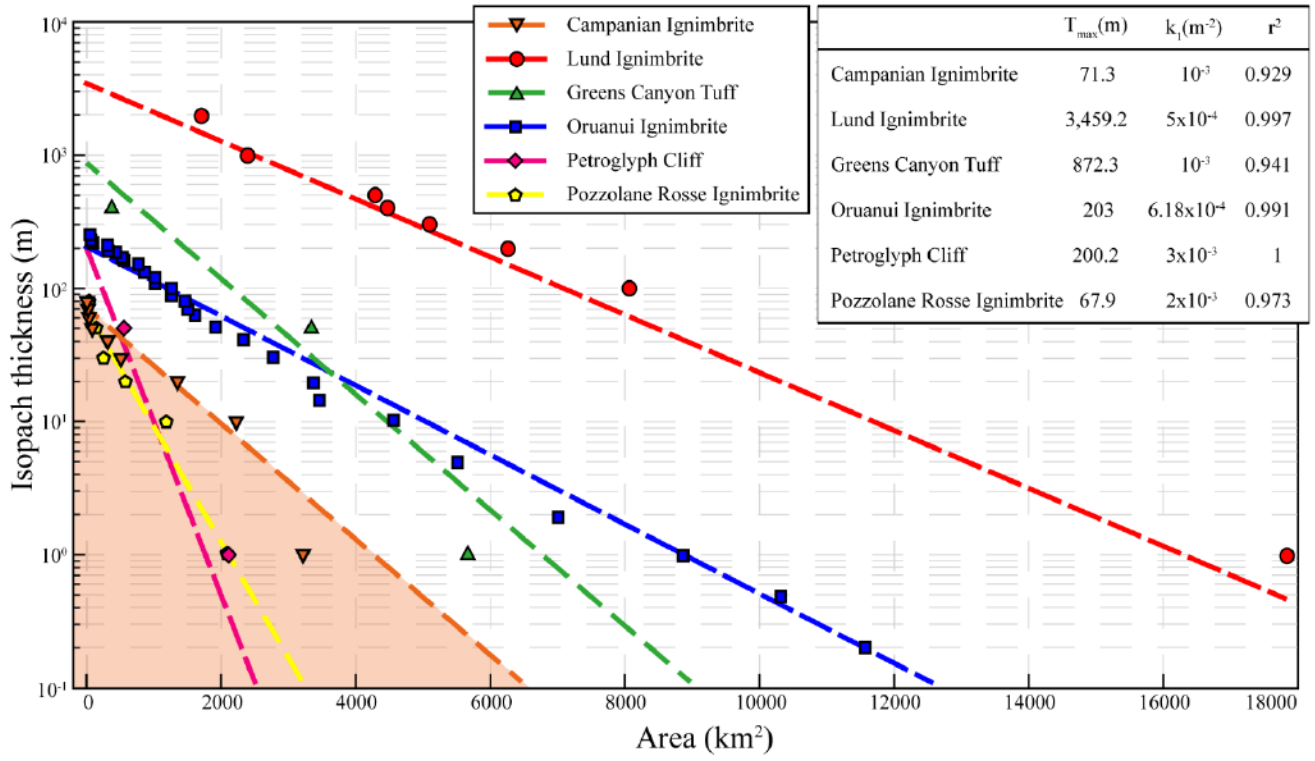

	T_{max}(m)	k_1(m^{-2})	r^2
Campanian Ignimbrite	71.3	10^{-3}	0.929
Lund Ignimbrite	3,459.2	$5x10^{-4}$	0.997
Greens Canyon Tuff	872.3	10^{-3}	0.941
Oruanui Ignimbrite	203	$6.18x10^{-4}$	0.991
Petroglyph Cliff	200.2	$3x10^{-3}$	1
Pozzolane Rosse Ignimbrite	67.9	$2x10^{-3}$	0.973

Figure 7. *Thickness (in log scale) versus the cumulative area enclosed in that thickness of each isopach of different ignimbrites (the CI in orange; the Lund Ignimbrite in red, Best et al., 2013a; the Greens Canyon Tuff in green, Best et al., 2013a; the Oruanui Ignimbrite in blue, Wilson, 1991; the Petroglyph Cliff in pink, Best et al., 2013a; and the Pozzolane Rosse Ignimbrite in yellow, Giordano and Doronzo, 2017). The dashed lines represent the fit of each ignimbrite. The values of the fitting (T_{max}, k_1, and r^2) are reported in the upper right corner. The plotted CI points are those obtained by the isopach map. The CI volume is the integrated area displayed in orange.*

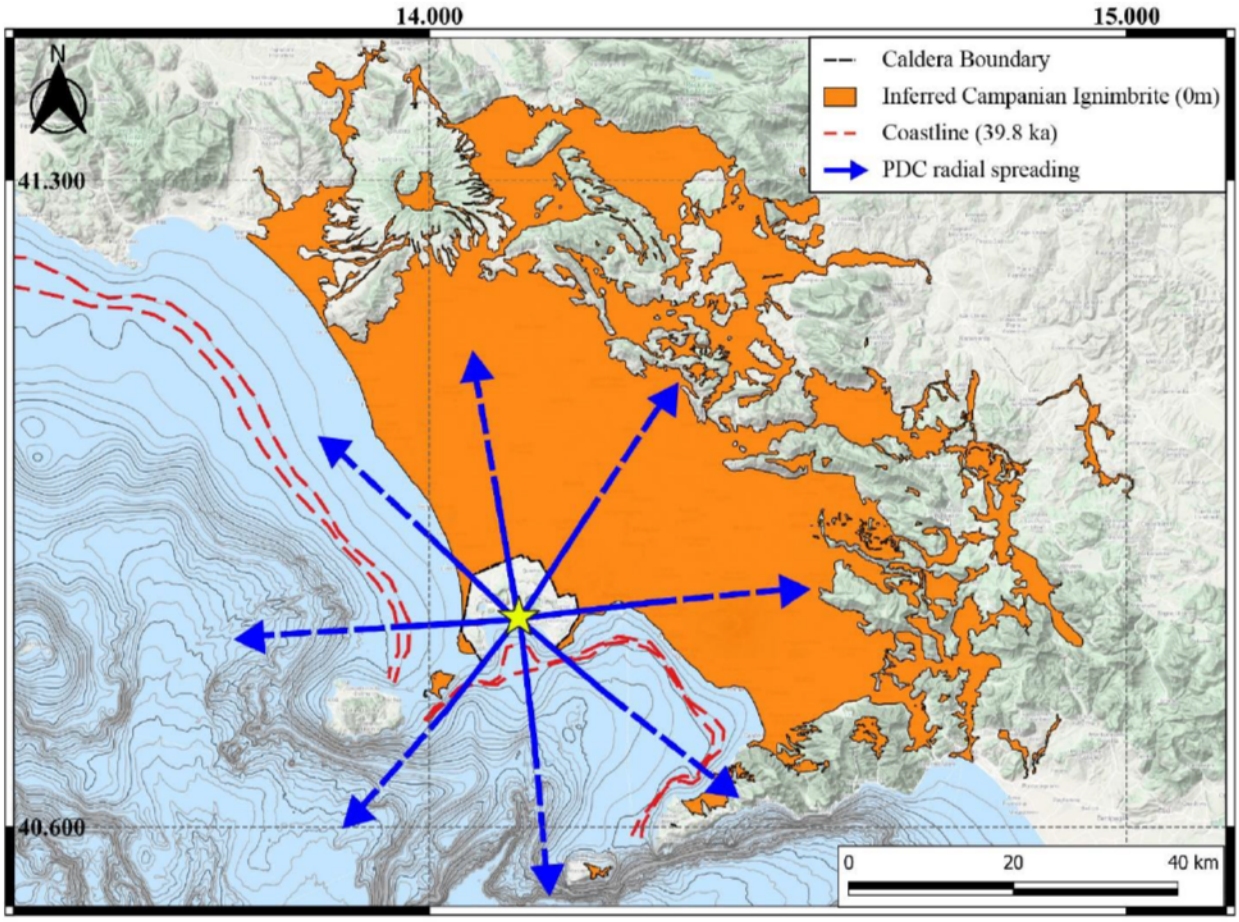

724

725 ***Figure 8.*** *Bathymetry of the submerged area of the Campi Flegrei Caldera. The red line is the 40 ka*
726 *coastline, equivalent to -75 – -87 m of the present one. The blue arrows indicate the possible radial*
727 *spreading of the PDC based on outcrops disposed radially from the center of the Caldera (yellow*
728 *star) and turbidity currents in the Tyrrhenian Sea. Accumulation of volume south of the caldera is*
729 *credible, due to the large submarine depressions and valleys.*

730 **3.2 Tables**

731 ***Table 1.*** *Bulk and DRE (*) volume calculations proposed for the CI eruption by different authors. Y-*
732 *5 refers to those studies that did not identify the co-Plinian and co-ignimbrite contribution. The*
733 *methods are described in the text. The used density (kg/m^3) is reported bulk or DRE (*), i: ignimbrite,*
734 *a: ash, p: pumices.*

735

Volume calculations (km^3)							
Plinian fallout	Co-Plinian ash	PDC	Co-ignimbrite ash	Y-5	Total	**Authors**	**Used density (kg/m^3)**
5.33 (0.88*)	14.67 (6.88*)					Scarpati and Perrotta, 2016	1,000 (2,400*)
4	16		100			Perrotta and Scarpati, 2003	
		54 (25*)	100 (42*)			Scarpati et al., 2014	2,600*
		30-40*		100 (30-40*)	60-80*	Thunell et al., 1979	

15				Rosi et al., 1999	
		73	>150	Cornell et al., 1983	
54 (22.6*)	153.9 (61.6*)		207.9 (84.2*)	Marti et al., 2016	2,500*
	72-120 (31-50*)		105-210*	Pyle et al., 2006	2,400*
25*	120*		145*	Civetta et al., 1997	
20*	130*		150*	Marianelli et al., 2006	
			200*	Fedele et al., 2003	~1,250
	180	140	320 (200*)	Rolandi et al., 2003	
20*	180*		200*	Pappalardo et al., 2008	Average porosity: 0.58
		250-300 (104-125*)	430-680 (180-280*)	Costa et al., 2012	1,000
10 (3*)	385 (215*)	180 (86*)	575 (300*)	Giaccio, 2006	1,400-2,500 l, 1,200 a, 800 p
	500			Fisher et al., 1993	

736

737 ***Table 2.*** *The values of thickness (m), area (km^2), cumulative area (km^2), volume (km^3), cumulative*
738 *volume (km^3) and the percentage of volume for each isopach.*

739

Thickness (m)	Area (km^2)	Cumulative area (km^2)	Volume (km^3)	Cumulative volume (km^3)	Volume (%)
>80	12.6	12.6	0.9	0.9	1.3
70-79	12.3	24.9	0.9	1.8	1.3
60-69	19.1	44.0	1.3	3.1	1.9
50-59	31.3	75.3	2.1	5.2	3.1
40-49	234.0	309.4	13.8	19.0	20.2
30-39	194.5	503.9	9.2	28.2	13.6
20-29	854.0	1,357.9	24.7	53.0	36.3
10-19	862.0	2,219.9	10.6	63.6	15.5
0-9	995.7	3,215.6	4.6	68.2	6.8
Total	**3,215.6**		**68.2**		

740

741 ***Table 3.*** *The volume of the CI eruption. The various parts of the PDC volume estimate are explained*
742 *in the text. The fallout volume considered in this work is the maximum and the minimum proposed in*
743 *literature by Perrotta and Scarpati (2003) and Marti et al. (2016).*

744

	Bulk Volume (km^3)	DRE Volume (km^3)
Preserved extra-caldera ignimbrite volume (V_{pr})	62 – 75	24 – 29
Marine volume (V_m)	62 – 75	24 – 29

Intracaldera volume (V_{intr})	16 – 43	8 – 21
Areal erosion volume (V_e)	10	4
Co-ignimbrite ash volume (V_{coign})	294 – 394	116 – 155
Total PDC volume (V_{pdc})	453 – 606	176 – 243
Fallout volume (V_{Pfall}) (Perrotta and Scarpati, 2003; Marti et al., 2016)	4 – 54	2 – 23
Total CI volume (V)	457 – 660	177 – 265

4 Nomenclature

Abbreviations and acronyms

a.s.l.: above sea level; CCDB: Collapse Caldera Database; CE: Common Era; CF: Campi Flegrei; CI: Campanian Ignimbrite; DEM: Digital Elevation Model; DRE: Dense Rock Equivalent; ka: thousands of years ago; kyrs: thousand years; GCT: Greens Canyon Tuff; LAMEVE: Large Magnitude Explosive Volcanic Eruptions, https://www.bgs.ac.uk/vogripa/view/controller.cfc?method=lameve; LYT: Lithified Yellow Tuff; M: Magnitude; NYT: Neapolitan Yellow Tuff; PDC: Pyroclastic Density Current; RED: Pozzolane Rosse Ignimbrite; USAF: Unconsolidated Stratified Ash Flow; V: total volume; V_{coign}: co-ignimbrite ash fall volume; V_{Pcol}: volume ejected during the phases that produced Plinian columns; $V_{coPfall}$: co-Plinian fall volume; V_e: areal erosion volume; VEI: Volcanic Explosivity Index; V_g: geometric volume; V_{ign}: ignimbrite volume; V_{intr}: intracaldera volume; V_m: marine volume; V_{mx}: matrix volume; V_{pdc}: pyroclastic density current volume; V_{Pfall}: proximal pumice lapilli deposits volume; V_{pr}: preserved extra-caldera bulk volume; WGI: Welded Gray Ignimbrite; ρ: bulk density; φ_t: total porosity.

5 Conflict of Interest

The authors declare that the research was conducted in the absence of any commercial or financial relationships that could be construed as a potential conflict of interest.

6 Author Contributions

AS conducted fieldwork, analysis, wrote the draft of this manuscript and made the figures. GG designed the research and helped in the development of the method. RI contributed to data collection. All the authors contributed to the fieldwork, reviewed and edited the draft.

7 Funding

AS and GG gratefully acknowledge The Grant of Excellence Departments, MIUR-Italy. Partial support was provided by NSF EAR1761713 to MHO and AS.

8 Acknowledgments

AS and GG gratefully acknowledge The Grant of Excellence Departments, MIUR-Italy. AS thanks Emanuele Sciarrino and Rose Gallo for their help in the fieldwork. Partial support was provided by NSF EAR1761713 to MHO and AS. We thank Danilo M. Palladino and Antonio Costa for discussions that improved an earlier version of this paper. Colin J. N. Wilson, Samantha Engwell, as well as an anonymous reviewer and the editor Pablo Tierz are acknowledged for helpful comments that have highly improved the manuscript.

9 References

Acocella, V. (2008). Activating and reactivating pairs of nested collapses during caldera-forming eruptions: Campi Flegrei (Italy). ***Geophys. Res. Lett.*** 35, L17304. doi:10.1029/2008GL035078

Albert, P. G., Giaccio, B., Isaia, R., Costa, A., Niespolo, E. M., Nomade, S., et al. (2019). Evidence for a large-magnitude eruption from Campi Flegrei caldera (Italy) at 29 ka. ***Geology*** 47, 595–599. doi:10.1130/G45805.1

Aldiss, D. T., and Ghazali, S. A. (1984). The regional geology and evolution of the Toba volcano-tectonic depression, Indonesia. ***J. Geol. Soc. London*** 141, 487–500. doi:10.1144/gsjgs.141.3.0487

Allen, S. R., and Cas, R. A. F. (2001). Transport of pyroclastic flows across the sea during the explosive, rhyolitic eruption of the Kos Plateau Tuff, Greece. ***Bull. Volcanol.*** 62, 441–456. doi:10.1007/s004450000107

Andrews, B. J., and Manga, M. (2011). Effects of topography on pyroclastic density current runout and formation of coignimbrites. ***Geology*** 39, 1099–1102. doi:10.1130/G32226.1

Antonioli, F. (2012). Sea level change in Western-Central Mediterranean since 300 kyr: comparing global sea level curves with observed data. ***Alp. Mediterr. Quat.*** 25, 15–23.

Antonioli, F., Bard, E., Potter, E. K., Silenzi, S., and Improta, S. (2004). 215-ka history of sea-level oscillations from marine and continental layers in Argentarola Cave speleothems (Italy). ***Glob. Planet. Change*** 43, 57–78. doi:10.1016/j.gloplacha.2004.02.004

Auker, M. R., Sparks, R. S. J., Siebert, L., Crosweller, H. S., and Ewert, J. (2013). A statistical analysis of the global historical volcanic fatalities record. ***J. Appl. Volcanol.*** 2, 2. doi:10.1186/2191-5040-2-2

Badino, F., Pini, R., Ravazzi, C., Margaritora, D., Arrighi, S., Bortolini, E., et al. An overview of Alpine and Mediterranean palaeogeography, terrestrial ecosystems and climate history during MIS 3 with focus on the Middle to Upper Palaeolithic transition. ***Quat. Int.*** In press. doi:10.1016/j.quaint.2019.09.024

Barberi, F., Innocenti, F., Lirer, L., Munno, R., Pescatore, T., and Santacroce, R. (1978). The Campanian Ignimbrite: a Major Prehistoric Eruption in the Neapolitan area (Italy). ***Bull. Volcanol.*** 41, 10–31. doi:10.1007/BF02597680

Bellucci, F. (1994). Nuove conoscenze stratigrafiche sui depositi vulcanici del sottosuolo del settore

meridionale della Piana Campana. ***Boll. Soc. Geol. It.*** 113, 395–420.

Best, M. G., Christiansen, E. H., Deino, A. L., Gromme, S., Hart, G. L., and Tingey, D. G. (2013a). The 36-18 Ma Indian Peak-Caliente ignimbrite field and calderas, southeastern Great Basin, USA: Multicyclic super-eruptions. ***Geosphere*** 9, 864–950. doi:10.1130/GES00902.1

Best, M. G., Gromme, S., Deino, A. L., Christiansen, E. H., Hart, G. L., and Tingey, D. G. (2013b). The 36-18 Ma Central Nevada ignimbrite field and calderas, Great Basin, USA: Multicyclic super-eruptions. ***Geosphere*** 9, 1562–1636. doi:10.1130/GES00945.1

Black, B. A., Neely, R. R., and Manga, M. (2015). Campanian Ignimbrite volcanism, climate, and the final decline of the Neanderthals. ***Geology*** 43, 411–414. doi:10.1130/G36514.1

Bonadonna, C., Ernst, G. G. J., and Sparks, R. S. J. (1998). Thickness variations and volume estimates of tephra fall deposits: the importance of particle Reynolds number. ***J. Volcanol. Geotherm. Res.*** 81, 173–187. doi:10.1016/S0377-0273(98)00007-9

Bonadonna, C., and Houghton, B. F. (2005). Total grain-size distribution and volume of tephra-fall deposits. ***Bull. Volcanol.*** 67, 441-456. doi:10.1007/s00445-004-0386-2

Bonadonna, C., and Phillips, J. C. (2003). Sedimentation from strong volcanic plumes. ***J. Geophys. Res.*** 108, 2340. doi:10.1029/2002jb002034

Brown, S. K., Jenkins, S. F., Sparks, R. S. J., Odbert, H., and Auker, M. R. (2017). Volcanic fatalities database: analysis of volcanic threat with distance and victim classification. ***J. Appl. Volcanol.*** 6, 15. doi:10.1186/s13617-017-0067-4

Broxton, D., and Reneau, S. (1996). "Buried early Pleistocene landscapes beneath the Pajarito Plateau, Northern New Mexico," in The Jemez Mountains Region. New Mexico Geological Society 47th Field Conference Guidebook, eds F. Goff, B. S. Kues, M. A. Rogers, L. D. McFadden and J. N. Gardner, 325–334.

Burden, R. E., Chen, L., and Phillips, J. C. (2013). A statistical method for determining the volume of volcanic fall deposits. ***Bull. Volcanol.*** 75, 707. doi: 10.1007/s00445-013-0707-4

Bursik, M. I., and Woods, A. W. (2000). The effects of topography on sedimentation from particle-laden turbulent density currents. ***J. Sediment. Res.*** 70, 53–63. doi:10.1306/2DC408FE-0E47-11D7-8643000102C1865D

Cappelletti, P., Cerri, G., Colella, A., de'Gennaro, M., Langella, A., Perrotta, A., et al. (2003). Post-eruptive processes in the Campanian Ignimbrite. ***Mineral. Petrol.*** 79, 79–97. doi:10.1007/s00710-003-0003-7

Carey, S. N., Sigurdsson, H., Mandeville, C., and Bronto, S. (1996). Pyroclastic flows and surges over water: an example from the 1883 Krakatau eruption. ***Bull. Volcanol.*** 57, 493–511. doi:10.1007/BF00304435

Cini Castagnoli, G., Albrecht, A., Beer, J., Shen, C., Callegari, E., Taricco, C., et al. (1995). Evidence for enhanced ^{10}Be deposition in Mediterranean sediments 35 Kyr BP. ***Geophys. Res. Lett.*** 22, 707–710. doi:10.1029/95GL00298

Civetta, L., Orsi, G., Pappalardo, L., Fisher, R. V., Heiken, G., and Ort, M. H. (1997). Geochemical zoning, mingling, eruptive dynamics and depositional processes - the Campanian Ignimbrite, Campi Flegrei caldera, Italy. ***J. Volcanol. Geotherm. Res.*** 75, 183–219. doi:10.1016/S0377-0273(96)00027-3

Cook, G. W., Wolff, J. A., and Self, S. (2016). Estimating the volume of a large pyroclastic body: the Otowi Member of the Bandelier Tuff, Valles caldera, New Mexico. ***Bull. Volcanol.*** 78, 10. doi:10.1007/s00445-016-1000-0

Cornell, W., Carey, S. N., and Sigurdsson, H. (1983). Computer simulation of transport and deposition of the campanian Y-5 ash. ***J. Volcanol. Geotherm. Res.*** 17, 89–109. doi:10.1016/0377-0273(83)90063-X

Costa, A., Folch, A., Macedonio, G., Giaccio, B., Isaia, R., and Smith, V. C. (2012). Quantifying volcanic ash dispersal and impact of the Campanian Ignimbrite super-eruption. ***Geophys. Res. Lett.*** 39, L10310. doi:10.1029/2012GL051605

Costa, A., Suzuki, Y. J., and Koyaguchi, T. (2018). Understanding the plume dynamics of explosive super-eruptions. ***Nat. Commun.*** 9, 654. doi:10.1038/s41467-018-02901-0

Crosweller, H. S., Arora, B., Brown, S. K., Cottrell, E., Deligne, N. I., Guerrero, N. O., et al. (2012). Global database on large magnitude explosive volcanic eruptions (LaMEVE). ***J. Appl. Volcanol.*** 1, 4. doi:10.1186/2191-5040-1-4

Cutler, N. A., Streeter, R. T., Engwell, S. L., Bolton, M. S., Jensen, B. J. L. and Dugmore, A. J. (2020). How does tephra deposit thickness change over time? A calibration exercise based on the 1980 Mount St Helens tephra deposit. ***J. Volcanol. Geotherm. Res.*** 399, 106883. doi:10.1016/j.jvolgeores.2020.106883

Daag, A., and van Westen, C. J. (1996). Cartographic modelling of erosion in pyroclastic flow deposits of Mount Pinatubo, Philippines. ***ITC Journal*** 2, 110-124.

De Natale, G., Troise, C., Mark, D., Mormone, A., Piochi, M., Di Vito, M. A., et al. (2016). The Campi Flegrei Deep Drilling Project (CFDDP): New insight on caldera structure, evolution and hazard implications for the Naples area (Southern Italy). ***Geochem. Geophys. Geosyst.*** 17, 4836–4847. doi:10.1002/2015GC006183

De Vivo, B., Rolandi, G., Gans, P. B., Calvert, A., Bohrson, W. A., Spera, F. J., et al. (2001). New constraints on the pyroclastic eruptive history of the Campanian volcanic Plain (Italy). ***Mineral. Petrol.*** 73, 47–65. doi:10.1007/s007100170010

Di Vito, M. A., Isaia, R., Orsi, G., Southon, J., de Vita, S., D'Antonio, M., et al. (1999). Volcanism and deformation since 12,000 years at the Campi Flegrei caldera (Italy). ***J. Volcanol. Geotherm. Res.*** 91, 221–246. doi:10.1016/S0377-0273(99)00037-2

Douka, K., Higham, T. F., Wood, R., Boscato, P., Gambassini, P., Karkanas, P., et al. (2014). On the chronology of the Uluzzian. ***J. Hum. Evol.*** 68, 1-13. doi:10.1016/j.jhevol.2013.12.007

Dufek, J., and Bergantz, G. W. (2007). Dynamics and deposits generated by the Kos Plateau Tuff eruption: Controls of basal particle loss on pyroclastic flow transport. ***Geochem., Geophys.***

882 *Geosystems* 8, Q12007. doi:10.1029/2007GC001741

883 Engwell, S. L., Aspinall, W. P., and Sparks, R. S. J. (2015). An objective method for the production
884 of isopach maps and implications for the estimation of tephra deposit volumes and their
885 uncertainties. ***Bull. Volcanol.*** 77, 61. doi:10.1007/s00445-015-0942-y

886 Engwell, S. L., Sparks, R. S. J., and Carey, S. N. (2014). Physical characteristics of tephra layers in
887 the deep sea realm: the Campanian Ignimbrite eruption. ***Geol. Soc. London, Spec. Publ.*** 398,
888 47–64. doi:10.1144/SP398.7

889 Fedele, F. G., Giaccio, B., Isaia, R., and Orsi, G. (2002). Ecosystem Impact of the Campanian
890 Ignimbrite Eruption in Late Pleistocene Europe. ***Quat. Res.*** 57, 420–424.
891 doi:10.1006/qres.2002.2331

892 Fedele, F. G., Giaccio, B., Isaia, R., and Orsi, G. (2003). The Campanian Ignimbrite Eruption,
893 Heinrich Event 4, and Palaeolithic Change in Europe: a High-Resolution Investigation. ***AGU***
894 ***Geophys. Monograph*** 139, 301–325. doi:10.1029/139GM20

895 Fedele, F. G., Giaccio, B., Isaia, R., Orsi, G., Carroll, M. R., and Scaillet, B. (2007). "The Campanian
896 Ignimbrite Factor: Towards a Reappraisal of the Middle to Upper Palaeolithic 'Transition'," in
897 Living Under the Shadow: Cultural Impacts of Volcanic Eruptions, eds J. Grattan and R.
898 Torrence (Walnutt Creek, CA: Left Coast Press), 19–41.

899 Fedele, L., Scarpati, C., Lanphere, M., Melluso, L., Morra, V., Perrotta, A., et al. (2008). The Breccia
900 Museo formation, Campi Flegrei, southern Italy: geochronology, chemostratigraphy and
901 relationship with the Campanian Ignimbrite eruption. ***Bull. Volcanol.*** 70, 1189–1219.
902 doi:10.1007/s00445-008-0197-y

903 Fedele, L., Scarpati, C., Sparice, D., Perrotta, A., and Laiena, F. (2016). A chemostratigraphic study
904 of the Campanian Ignimbrite eruption (Campi Flegrei, Italy): Insights on magma chamber
905 withdrawal and deposit accumulation as revealed by compositionally zoned stratigraphic and
906 facies framework. ***J. Volcanol. Geotherm. Res.*** 324, 105–117.
907 doi:10.1016/j.jvolgeores.2016.05.019

908 Fierstein, J., and Hildreth, W. (1992). The plinian eruptions of 1912 at Novarupta, Katmai National
909 Park, Alaska. ***Bull. Volcanol.*** 54, 646–684. doi:10.1007/BF00430778

910 Fisher, R. V., Orsi, G., Ort, M. H., and Heiken, G. (1993). Mobility of a large-volume pyroclastic
911 flow — emplacement of the Campanian ignimbrite, Italy. ***J. Volcanol. Geotherm. Res.*** 56, 205–
912 220. doi:10.1016/0377-0273(93)90017-L

913 Folch, A. (2012). A review of tephra transport and dispersal models: Evolution, current status, and
914 future perspectives. ***J. Volcanol. Geotherm. Res.*** 235–236, 96–115.
915 doi:10.1016/j.jvolgeores.2012.05.020

916 Folch, A., Costa, A., Durant, A., and Macedonio, G. (2010). A model for wet aggregation of ash
917 particles in volcanic plumes and clouds: 2. Model application. ***J. Geophys. Res.*** 115, B09202.
918 doi:10.1029/2009JB007176

919 Folkes, C. B., Wright, H. M. N., Cas, R. A. F., de Silva, S. L., Lesti, C., and Viramonte, J. G. (2011).

A re-appraisal of the stratigraphy and volcanology of the Cerro Galán volcanic system, NW Argentina. ***Bull. Volcanol.*** 73, 1427–1454. doi:10.1007/s00445-011-0459-y

Gambassini, P. (1997). ***Il Paleolitico di Castelcivita: culture e ambiente***. Napoli: Electa.

Geyer, A., and Martí, J. (2008). The new worldwide collapse caldera database (CCDB): A tool for studying and understanding caldera processes. ***J. Volcanol. Geotherm. Res.*** 175, 334–354. doi:10.1016/j.jvolgeores.2008.03.017

Giaccio, B. (2006). L'eruzione dell'Ignimbrite Campana (c. 40 ka BP), oscillazioni climatiche sub-orbitali e i cambiamenti bioculturali dell'OIS 3 europeo. [doctoral dissertation/PhD thesis]. [Naples (IT)]: University of Naples Federico II.

Giaccio, B., Hajdas, I., Isaia, R., Deino, A. L., and Nomade, S. (2017). High-precision ^{14}C and $^{40}Ar/^{39}Ar$ dating of the Campanian Ignimbrite (Y-5) reconciles the time-scales of climatic-cultural processes at 40 ka. ***Sci. Rep.*** 7, 45940. doi:10.1038/srep45940

Giaccio, B., Hajdas, I., Peresani, M., Fedele, F. G., and Isaia, R. (2006). "The Campanian Ignimbrite tephra and its relevance for the timing of the Middle to Upper Paleolithic shift," in When Neanderthals and modern humans met, ed N. J. Conard (Tübingen, Germany: Kerns Verlag.), 343–375.

Giaccio, B., Isaia, R., Fedele, F. G., Di Canzio, E., Hoffecker, J. F., Ronchitelli, A., et al. (2008). The Campanian Ignimbrite and Codola tephra layers: Two temporal/stratigraphic markers for the Early Upper Palaeolithic in southern Italy and eastern Europe. ***J. Volcanol. Geotherm. Res.*** 177, 208–226. doi:10.1016/j.jvolgeores.2007.10.007

Giordano, G. (1998). The effect of paleotopography on lithic distribution and facies associations of small volume ignimbrites: the WTT Cupa (Roccamonfina volcano, Italy). ***J. Volcanol. Geotherm. Res.*** 87, 255–273. doi:10.1016/ S0377-0273(98)00096-1

Giordano, G., and Doronzo, D. M. (2017). Sedimentation and mobility of PDCs: a reappraisal of ignimbrites' aspect ratio. ***Sci. Rep.*** 7, 4444. doi:10.1038/s41598-017-04880-6

Giordano, G. and the CARG team (2010). "Stratigraphy and volcano-tectonic structures of the Colli Albani volcanic field," in The Colli Albani Volcano, eds R. Funiciello and G. Giordano, vol. Geol. Soc. London, Special Publication of IAVCEI 3, 43–97.

Hajdas, I., Taricco, C., Bonani, G., Beer, J., Bernasconi, S. M., and Wacker, L. (2011). Anomalous radiocarbon ages found in Campanian Ignimbrite deposit of the Mediterranean deep-sea core CT85-5. ***Radiocarbon*** 53, 575–583. doi:10.1017/S0033822200039059

Henry, C. D., and Price, J. G. (1984). Variations in caldera development in the Tertiary volcanic field of Trans-Pecos Texas. ***J. Geophys. Res.*** 89, 8765–8786. doi:10.1029/JB089iB10p08765

Isaia, R., Marianelli, P., and Sbrana, A. (2009). Caldera unrest prior to intense volcanism in Campi Flegrei (Italy) at 4.0 ka B.P.: Implications for caldera dynamics and future eruptive scenarios. ***Geophys. Res. Lett.*** 36, L21303. doi:10.1029/2009GL040513

ISPRA (2009). Geological Map n. 432 ''Benevento''; scale 1:50,000. National Geological Survey of

Italy, Università degli studi di Urbino, Istituto di Geologia Applicata, Urbino, Italy.

ISPRA (2010). Geological Map n. 431 ''Caserta Est''; scale 1:50,000. National Geological Survey of Italy, Regione Campania, Settore Difesa Suolo, Napoli, Italy.

ISPRA (2011a). Geological Map n. 465 ''Isola di Procida''; scale 1:50,000. National Geological Survey of Italy, Regione Campania, Settore Difesa Suolo, Napoli, Italy.

ISPRA (2011b). Geological Map n. 448 ''Ercolano''; scale 1:50,000. National Geological Survey of Italy, CNR Consiglio Nazionale delle Ricerche, Italy.

ISPRA (2011c). Geological Map n. 467 ''Salerno''; scale 1:50,000. National Geological Survey of Italy, (http://www.isprambiente.gov.it/MEDIA/carg/ campania.html).

ISPRA (2011d). Geological Map n. 446-447 ''Napoli''; scale 1:50,000. National Geological Survey of Italy, Regione Campania - Settore Difesa Suolo, Napoli, Italy.

ISPRA (2014a). Geological Map n. 450 ''S.Angelo dei Lombardi''; scale 1:50,000. National Geological Survey of Italy, CNR Consiglio Nazionale delle Ricerche, Italy.

ISPRA (2014b). Geological Map n. 466-485 ''Sorrento-Termini''; scale 1:50,000. National Geological Survey of Italy, CNR Consiglio Nazionale delle Ricerche, Italy.

ISPRA (2016). Geological Map n. 449 ''Avellino''; scale 1:50,000. National Geological Survey of Italy, Regione Campania, Italy.

ISPRA (2018). Geological Map n. 464 ''Isola d'Ischia''; scale 1:25,000. National Geological Survey of Italy, Regione Campania, Settore Difesa Suolo, Napoli, Italy.

Keller, J., Ryan, W. B. F., Ninkovich, D., and Altherr, R. (1978). Explosive volcanic activity in the Mediterranean over the past 200,000 yr as recorded in deep-sea sediments. ***Bull. Geol. Soc. Am.*** 89, 591–604. doi:10.1130/0016-7606(1978)89<591:EVAITM>2.0.CO;2

Lambeck, K., and Bard, E. (2000). Sea-level change along the French Mediterranean coast for the past 30000 years. ***Earth Planet. Sci. Lett.*** 175, 203–222. doi:10.1016/S0012-821X(99)00289-7

Langella, A., Bish, D. L., Calcaterra, D., and Cappelletti, P. (2013). "L'Ignimbrite Campana (IC)," in **Le pietre storiche della Campania dall'oblio alla riscoperta**, eds M. De Gennaro, D. Calcaterra and A. Langella (Napoli: Luciano Editore), 155–177.

Lowe, J., Barton, N., Blockley, S., Ramsey, C. B., Cullen, V. L., Davies, W., et al. (2012). Volcanic ash layers illuminate the resilience of Neanderthals and early modern humans to natural hazards. ***Proc. Natl. Acad. Sci.*** 109, 13532–13537. doi:10.1073/pnas.1204579109

Marianelli, P., Sbrana, A., and Proto, M. (2006). Magma chamber of the Campi Flegrei supervolcano at the time of eruption of the Campanian Ignimbrite. ***Geology*** 34, 937-940. doi:10.1130/G22807A.1

Marti, A., Folch, A., Costa, A., and Engwell, S. L. (2016). Reconstructing the plinian and co-ignimbrite sources of large volcanic eruptions: A novel approach for the Campanian Ignimbrite. ***Sci. Rep.*** 6, 21220. doi:10.1038/srep21220

Mason, B. G., Pyle, D. M., and Oppenheimer, C. (2004). The size and frequency of the largest explosive eruptions on Earth. ***Bull. Volcanol.*** 66, 735–748. doi:10.1007/s00445-004-0355-9

McCoy, F.W., and Cornell, W. (1990). "Volcaniclastic sediments in the Tyrrhenian Basin," in Proceedings of the Ocean Drilling Program, Scientific Results 107, eds K. A. Kastens, J. Mascle et al. (Swindon, UK: ODP, Texas A&M University, College Station, UK distributors, IPOD Committee, NERC), 291-305. doi:10.2973/odp.proc.sr.107.119.1990

Melekestsev, I. V., Kirianov, V. Y., and Praslov, N. D. (1984). Catastrophic eruption in the Phlegrean Fields region (Italy) - possible source for a volcanic ash in late Pleistocene sediments on the European part of the USSR. ***Vulcanol. i Seismol.*** 3, 35–44.

Melluso, L., Morra, V., Perrotta, A., Scarpati, C., and Adabbo, M. (1995). The eruption of the Breccia Museo (Campi Flegrei, Italy): Fractional crystallization processes in a shallow, zoned magma chamber and implications for the eruptive dynamics. ***J. Volcanol. Geotherm. Res.*** 68, 325–339. doi:10.1016/0377-0273(95)00020-5

Mihailović, D., and Whallon, R. (2017). Crvena Stijena revisited: the late Mousterian assemblages. ***Quat. Int.*** 450, 36-49. doi:10.1016/j.quaint.2016.12.026

Milia, A., Morabito, S., and Petrosino, P. (2020). Late Pleistocene–Holocene climatic and volcanic events in the bathyal area of the Eastern Tyrrhenian Sea and the stratigraphic signature of the 39 ka Campanian Ignimbrite eruption. ***Global Planet. Change*** 185, 103074. doi:10.1016/j.gloplacha.2019.103074

Milia, A., and Torrente, M. M. (2007). The influence of paleogeographic setting and crustal subsidence on the architecture of ignimbrites in the Bay of Naples (Italy). ***Earth Planet. Sci. Lett.*** 263, 192–206. doi:10.1016/j.epsl.2007.08.004

Morgan, L. A., Doherty, D. J., and Leeman, W. P. (1984). Ignimbrites of the Eastern Snake River Plain: Evidence for major caldera-forming eruptions. ***J. Geophys. Res.*** 89, 8665–8678. doi:10.1029/JB089iB10p08665

Morley, M. W., and Woodward, J. C. (2011). The Campanian Ignimbrite at Crvena Stijena rockshelter in Montenegro. ***Quat. Res.*** 75, 683-696. doi:10.1016/j.yqres.2011.02.005

Mormone, A., Troise, C., Piochi, M., Balassone, G., Joachimski, M., and De Natale, G. (2015). Mineralogical, geochemical and isotopic features of tuffs from the CFDDP drill hole: Hydrothermal activity in the eastern side of the Campi Flegrei volcano (southern Italy). ***J. Volcanol. Geotherm. Res.*** 290, 39–52. doi:10.1016/j.jvolgeores.2014.12.003

Narcisi, B. (1996). Tephrochronology of a late quaternary lacustrine record from the Monticchio maar (Vulture volcano, southern Italy). ***Quat. Sci. Rev.*** 15, 155–165. doi:10.1016/0277-3791(95)00045-3

Narcisi, B., and Vezzoli, L. (1999). Quaternary stratigraphy of distal tephra layers in the Mediterranean - An overview. ***Glob. Planet. Change*** 21, 31–50. doi:10.1016/S0921-8181(99)00006-5

Newhall, C. G., and Self, S. (1982). The volcanic explosivity index (VEI) an estimate of explosive

1031 magnitude for historical volcanism. ***J. Geophys. Res. Oceans*** 87, 1231-1238.
1032 doi:10.1029/JC087iC02p01231

1033 Orsi, G., de Vita, S., and Di Vito, M. A. (1996). The restless, resurgent Campi Flegrei nested caldera
1034 (Italy): constraints on its evolution and configuration. ***J. Volcanol. Geotherm. Res.*** 74, 179–214.
1035 doi:10.1016/S0377-0273(96)00063-7

1036 Ort, M. H., Orsi, G., Pappalardo, L., and Fisher, R. V. (2003). Anisotropy of magnetic susceptibility
1037 studies of depositional processes in the Campanian Ignimbrite, Italy. ***Bull. Volcanol.*** 65, 55–72.
1038 doi:10.1007/s00445-002-0241-2

1039 Ortolani, F., and Aprile, F. (1985). Principali caratteristiche stratigrafiche e strutturali dei depositi
1040 superficiali della Piana Campana. ***Boll. Soc. Geol. It.*** 104, 195–206.

1041 Pacheco-Hoyos, J. G., Aguirre-Díaz, G. J., and Dávila-Harris, P. (2018). Boiling-over dense
1042 pyroclastic density currents during the formation of the ~ 100 km^3 Huichapan ignimbrite in
1043 Central Mexico: Stratigraphic and lithofacies analysis. ***J. Volcanol. Geotherm. Res.*** 349, 268–
1044 282. doi:10.1016/j.jvolgeores.2017.11.007

1045 **Pappalardo, L., Civetta, L., D'Antonio, M., Deino, A. L., Di Vito, M. A., Orsi, G., et al. (1999).**
1046 Chemical and Sr-isotopical evolution of the Phlegraean magmatic system before the Campanian
1047 Ignimbrite and the Neapolitan Yellow Tuff eruptions. ***J. Volcanol. Geotherm. Res.*** 91, 141–166.
1048 doi:10.1016/S0377-0273(99)00033-5

1049 Pappalardo, L., Ottolini, L., and Mastrolorenzo, G. (2008). The Campanian Ignimbrite (southern
1050 Italy) geochemical zoning: insight on the generation of a super-eruption from catastrophic
1051 differentiation and fast withdrawal. ***Contrib. Mineral. Petrol.*** 156, 1–26. doi:10.1007/s00410-
1052 007-0270-0

1053 Parfitt, L., and Wilson, L. (2008). ***Fundamentals of Physical Volcanology***. Malden, USA: Blackwell.

1054 Paterne, M., Guichard, F., Labeyrie, J., Gillot, P. Y., and Duplessy, J. C. (1986). Tyrrhenian Sea
1055 tephrochronology of the oxygen isotope record for the past 60,000 years. ***Mar. Geol.*** 72, 259–
1056 285. doi:10.1016/0025-3227(86)90123-4

1057 Paterne, M., Kallel, N., Labeyrie, L., Vautravers, M., Duplessy, J. C., Rossignol-Strick, M., et al.
1058 (1999). Hydrological relationship between the North Atlantic Ocean and the Mediterranean Sea
1059 during the past 15 - 75 kyr. ***Paleoceanography*** 14, 626–638. doi:10.1029/1998PA900022

1060 Pérez, W., Alvarado, G. E., and Gans, P. B. (2006). The 322 ka Tiribí Tuff: stratigraphy,
1061 geochronology and mechanisms of deposition of the largest and most recent ignimbrite in the
1062 Valle Central, Costa Rica. ***Bull. Volcanol.*** 69, 25–40. doi:10.1007/s00445-006-0053-x

1063 Perrotta, A., and Scarpati, C. (1994). The dynamics of the Breccia Museo eruption (Campi Flegrei,
1064 Italy) and the significance of spatter clasts associated with lithic breccias. ***J. Volcanol.***
1065 ***Geotherm. Res.*** 59, 335–355. doi:10.1016/0377-0273(94)90086-8

1066 Perrotta, A., and Scarpati, C. (2003). Volume partition between the plinian and co-ignimbrite air fall
1067 deposits of the Campanian Ignimbrite eruption. ***Mineral. Petrol.*** 79, 67–78. doi:10.1007/s00710-
1068 003-0002-8

1069 Perrotta, A., Scarpati, C., Luongo, G., and Morra, V. (2006). "Chapter 5 The Campi Flegrei caldera
1070 boundary in the city of Naples," in Developments in Volcanology, eds B. De Vivo (Elsevier), 9,
1071 85–96. doi:10.1016/S1871-644X(06)80019-7

1072 Perrotta, A., Scarpati, C., Luongo, G., and Morra, V. (2010). Stratigraphy and volcanological
1073 evolution of the southwestern sector of Campi Flegrei and Procida Island, Italy. ***Geol. Soc. Am.***
1074 ***Spec. Pap.*** 464, 171–191. doi:10.1130/2010.2464(09)

1075 Pyle, D. M. (1989). The thickness, volume and grainsize of tephra fall deposits. ***Bull. Volcanol.*** 51,
1076 1–15. doi:10.1007/BF01086757

1077 **Pyle, D. M. (1990). "New volume estimates for the Minoan eruption of Santorini," in** Thera and the
1078 Aegean World III, eds D. A. Hardy, J. Keller, V. Galanopoulos, N. C. Flemming and T. H.
1079 Druitt (London: The Thera Foundation), 113–121.

1080 Pyle, D. M. (2000). "Sizes of volcanic eruptions," in The Encyclopedia of Volcanoes, eds H.
1081 Sigurdsson, B. F. Houghton, S. R. McNutt, H. Rymer and J. Stix (London: Academic Press),
1082 263–269.

1083 Pyle, D. M. (2015). "Sizes of volcanic eruptions," in The Encyclopedia of Volcanoes, ed H.
1084 Sigurdsson, B. F. Houghton, S. R. McNutt, H. Rymer and J. Stix (London: Academic Press),
1085 257–264. doi:10.1016/B978-0-12-385938-9.00013-4

1086 Pyle, D. M., Ricketts, G. D., Margari, V., van Andel, T. H., Sinitsyn, A. A., Praslov, N. D., et al.
1087 **(2006). Wide dispersal and deposition of distal tephra during the Pleistocene "Campanian**
1088 **Ignimbrite/Y5" eruption, Italy.** ***Quat. Sci. Rev.*** 25, 2713–2728.
1089 doi:10.1016/j.quascirev.2006.06.008

1090 Rampino, M. R., and Self, S. (1992). Volcanic winter and accelerated glaciation following the Toba
1091 super-eruption. ***Nature*** 359, 50–52. doi:10.1038/359050a0

1092 Ratté, J. C., Marvin, R. F., Naeser, C. W., and Bikerman, M. (1984). Calderas and ash flow tuffs of
1093 the Mogollon Mountains, southwestern New Mexico. ***J. Geophys. Res.*** 89, 8713.
1094 doi:10.1029/JB089iB10p08713

1095 Rhoades, D. A., Dowrick, D. J., and Wilson, C. J. N. (2002). Volcanic hazard in New Zealand:
1096 scaling and attenuation relations for tephra fall deposits from Taupo Volcano. ***Nat. Hazards*** 26,
1097 147–174. doi:10.1023/A:1015608732356

1098 Rolandi, G., Bellucci, F., Heizler, M. T., Belkin, H. E., and De Vivo, B. (2003). Tectonic controls on
1099 the genesis of ignimbrites from the Campanian Volcanic Zone, southern Italy. ***Mineral. Petrol.***
1100 79, 3–31. doi:10.1007/s00710-003-0014-4

1101 Rosi, M., and Sbrana, A. (1987). Phlegrean Fields. ***CNR, Quad. La Ricerca Sci.*** 114, 1–175.

1102 Rosi, M., Sbrana, A., and Principe, C. (1983). The Phlegraean Fields: structural evolution, volcanic
1103 history and eruptive mechanisms. ***J. Volcanol. Geotherm. Res.*** 17, 273–288. doi:10.1016/0377-
1104 0273(83)90072-0

1105 Rosi, M., Sbrana, A., and Vezzoli, L. (1988). Correlazioni tefrostratigrafiche di alcuni livelli di

1106 Ischia, Procida e Campi Flegrei. ***Mem. della Soc. Geol. Ital.*** 41, 1015–1027.

1107 Rosi, M., Vezzoli, L., Aleotti, P., and Censi, M. (1996). Interaction between caldera collapse and
1108 eruptive dynamics during the Campanian Ignimbrite eruption, Phlegraean Fields, Italy. ***Bull.***
1109 ***Volcanol.*** 57, 541–554. doi:10.1007/BF00304438

1110 Rosi, M., Vezzoli, L., Castelmenzano, A., and Grieco, G. (1999). Plinian pumice fall deposit of the
1111 Campanian Ignimbrite eruption (Phlegraean Fields, Italy). ***J. Volcanol. Geotherm. Res.*** 91, 179–
1112 198. doi:10.1016/S0377-0273(99)00035-9

1113 Ruberti, D., Vigliotti, M., Rolandi, R., and Di Lascio, M. (2020). "Effect of paleomorphology on
1114 facies distribution of the Campania Ignimbrite in the northern Campania Plain, southern Italy,"
1115 in Vesuvius, Campi Flegrei, and Campanian Volcanism, eds B. De Vivo, H. E. Belkin and G.
1116 Rolandi (Elsevier Inc.), 207–229. doi:10.1016/B978-0-12-816454-9.00009-2

1117 Scandone, R., Bellucci, F., Lirer, L., and Rolandi, G. (1991). The structure of the Campanian Plain
1118 and the activity of the Neapolitan volcanoes (Italy). ***J. Volcanol. Geotherm. Res.*** 48, 1–31.
1119 doi:10.1016/0377-0273(91)90030-4

1120 Scarpati, C., and Perrotta, A. (2012). Erosional characteristics and behavior of large pyroclastic
1121 density currents. ***Geology*** 40, 1035–1038. doi:10.1130/G33380.1

1122 Scarpati, C., and Perrotta, A. (2016). Stratigraphy and physical parameters of the Plinian phase of the
1123 Campanian Ignimbrite eruption. ***Bull. Geol. Soc. Am.*** 128, 1147–1159. doi:10.1130/B31331.1

1124 Scarpati, C., Perrotta, A., Lepore, S., and Calvert, A. (2013). Eruptive history of Neapolitan
1125 volcanoes : constraints from $^{40}Ar - ^{39}Ar$ dating. ***Geol. Mag.*** 150, 412–425.
1126 doi:10.1017/S0016756812000854

1127 Scarpati, C., Sparice, D., and Perrotta, A. (2014). A crystal concentration method for calculating
1128 ignimbrite volume from distal ash-fall deposits and a reappraisal of the magnitude of the
1129 Campanian Ignimbrite. ***J. Volcanol. Geotherm. Res.*** 280, 67–75.
1130 doi:10.1016/j.jvolgeores.2014.05.009

1131 Scarpati, C., Sparice, D., and Perrotta, A. (2015a). Facies variation in the Campanian Ignimbrite.
1132 ***Rend. Online Soc. Geol. Ital.*** 33, 83–87. doi:10.3301/ROL:2015.20

1133 Scarpati, C., Sparice, D., and Perrotta, A. (2015b). The ground layer of the Campanian Ignimbrite: an
1134 example of deposition from a dilute pyroclastic density current. ***Bull. Volcanol.*** 77, 97.
1135 doi:10.1007/s00445-015-0985-0

1136 Scott, W. E., Hoblitt, R. P., Torres, R. C., Self, S., Martinez, M. M. L., and Nillos, T. (1996).
1137 "Pyroclastic flows of the June 15, 1991, climactic eruption of Mount Pinatubo," in Fire and
1138 mud: Eruptions and lahars of Mount Pinatubo, Philippines, eds C.G. Newhall, and R.
1139 Punongbayan (Seattle: University of Washington Press), 545-570.

1140 Servizio Geologico d'Italia (1963). Carta geologica d'Italia scala 1:100.000, foglio 174 – Ariano
1141 Irpino "Geological map of Italy at 1:100.000 scale, sheet number 174 – Ariano Irpino". Servizio
1142 Geologico d'Italia, Rome.

Servizio Geologico d'Italia (1965). Carta geologica d'Italia scala 1:100.000, foglio 197 – Amalfi "Geological map of Italy at 1:100.000 scale, sheet number 197 – Amalfi". Servizio Geologico d'Italia, Rome.

Servizio Geologico d'Italia (1966). Foglio Geologico n°172 - Caserta. Carta Geologica d'Italia, scala 1:100.000, II ediz., Istituto Poligrafico e Zecca dello Stato, Roma.

Servizio Geologico d'Italia (1967). Carta geologica d'Italia scala 1:100.000, fogli 160 – Cassino "Geological map of Italy at 1:100.000 scale, sheet number 160 – Cassino". Servizio Geologico d'Italia, Rome.

Servizio Geologico d'Italia (1971a). Carta geologica d'Italia scala 1:100.000, foglio 171 – Gaeta e Vulcano di Roccamonfina "Geological map of Italy at 1:100.000 scale, sheet number 171 – Gaeta e Vulcano di Roccamonfina". Servizio Geologico d'Italia, Rome.

Servizio Geologico d'Italia (1971b). Carta geologica d'Italia scala 1:100.000, foglio 161 – Isernia "Geological map of Italy at 1:100.000 scale, sheet number 161 – Isernia". Servizio Geologico d'Italia, Rome.

Servizio Geologico d'Italia (1975). Carta geologica d'Italia scala 1:100.000, foglio 173 – Benevento "Geological map of Italy at 1:100.000 scale, sheet number 173 – Benevento". Servizio Geologico d'Italia, Rome.

Seymour, K. S., and Christanis, K. (1995). Correlation of a tephra layer in western Greece with a late Pleistocene eruption in the Campanian province of italy. ***Quat. Res.*** 43, 46–54. doi:10.1006/qres.1995.1005

Seymour, K. S., Christanis, K., Bouzinos, A., Papazisimou, S., Papatheodorou, G., Moran, E., et al. (2004). Tephrostratigraphy and tephrochronology in the Philippi peat basin, Macedonia, Northern Hellas (Greece). ***Quat. Int.*** 121, 53–65. doi:10.1016/j.quaint.2004.01.023

Smith, V. C., Isaia, R., Engwell, S. L., and Albert, P. G. (2016). Tephra dispersal during the Campanian Ignimbrite (Italy) eruption: implications for ultra-distal ash transport during the large caldera-forming eruption. ***Bull. Volcanol.*** 78, 45. doi:10.1007/s00445-016-1037-0

Smith, V. C., Isaia, R., and Pearce, N. J. G. (2011). Tephrostratigraphy and glass compositions of post-15 kyr Campi Flegrei eruptions: Implications for eruption history and chronostratigraphic markers. ***Quat. Sci. Rev.*** 30, 3638–3660. doi:10.1016/j.quascirev.2011.07.012

Sparice, D. (2015). Definizione delle litofacies e ricostruzione dell'architettura dell'Ignimbrite Campana. [doctoral dissertation/PhD thesis]. [Naples (IT)]: University of Naples Federico II.

Sparks, R. S. J., Francis, P. W., Hamer, R. D., Pankhurst, R. J., O'Callaghan, L. O., Thorpe, R. S., et al. (1985). Ignimbrites of the Cerro Galan caldera, NW Argentina. ***J. Volcanol. Geotherm. Res.*** 24, 205–248. doi:10.1016/0377-0273(85)90071-X

Sparks, R. S. J., and Huang, T. C. (1980). The volcanological significance of deep-sea ash layer associated with ignimbrites. ***Geol. Mag.*** 117, 425–436. doi:10.1017/S0016756800028533

Sparks, R. S. J., and Walker, G. P. L. (1977). The significance of vitric-enriched air-fall ashes

associated with crystal-enriched ignimbrites. ***J. Volcanol. Geotherm. Res.*** 2, 329–341. doi:10.1016/0377-0273(77)90019-1

Sparks, R. S. J., Self, S., Grattan, J., Oppenheimer, C., Pyle, D. M., and Rymer, H. (2005). Super-eruptions: global effects and future threats. London. ***Report of a Geological Society of London Working Group***, (London, UK: The Geological Society).

Stuiver, M., Grootes, P. M., and Braziunas, T. F. (1995). The GISP2 $\delta^{18}O$ Climate Record of the Past 16,500 Years and the Role of the Sun, Ocean, and Volcanoes. ***Quat. Res.*** 44, 341–354. doi:10.1006/qres.1995.1079

Takarada, S. and Hoshizumi, H. (2020). Distribution and Eruptive Volume of Aso-4 Pyroclastic Density Current and Tephra Fall Deposits, Japan: A M8 Super-Eruption. ***Front. Earth Sci.*** 8:170. doi: 10.3389/feart.2020.00170

Tarquini, S., Isola, I., Favalli, M., Mazzarini, F., Bisson, M., Pareschi, M. T., et al. (2007). TINITALY/01: a new Triangular Irregular Network of Italy. ***Ann. Geophys.*** 50, 407 - 425.

Tarquini, S., and Nannipieri, L. (2017). The 10 m-resolution TINITALY DEM as a trans-disciplinary basis for the analysis of the Italian territory: Current trends and new perspectives. ***Geomorphology*** 281, 108-115. doi:10.1016/j.geomprph.2016.12.022

Tarquini, S., Vinci, S., Favalli, M., Doumaz, F., Fornaciai, A., and Nannipieri, L. (2012). Release of a 10-m-resolution DEM for the Italian territory: Comparison with global-coverage DEMs and anaglyph-mode exploration via the web. ***Comput. Geosci.*** 38, 168-170. doi:10.1016/j.cageo.2011.04.018

Thordarson, T., and Self, S. (1996). Sulfur, chlorine and fluorine degassing and atmospheric loading by the Roza eruption, Columbia River Basalt Group, Washington, USA. ***J. Volcanol. Geotherm. Res.*** 74, 49–73. doi:10.1007/s004450050136

Thunell, R., Federman, A., Sparks, R. S. J., and Williams, D. (1979). The Age, Origin, and Volcanological Significance of the Y-5 Ash Layer in the Mediterranean. ***Quat. Res.*** 12, 241–253. doi:10.1016/0033-5894(79)90060-7

Ton-That, T., Singer, B., and Paterne, M. (2001). $^{40}Ar/^{39}Ar$ dating of latest Pleistocene (41 ka) marine tephra in the Mediterranean Sea: implications for global climate records. ***Earth Planet. Sci. Lett.*** 184, 645–658. doi:10.1016/S0012-821X(00)00358-7

Torrente, M. M., Milia, A., Bellucci, F., and Rolandi, G. (2010). Extensional tectonics in the Campania Volcanic Zone (eastern Tyrrhenian Sea, Italy): new insights into the relationship between faulting and ignimbrite eruptions. ***Boll. Soc. Geol. It.*** 129, 297–315. doi:10.3301/IJG.2010.07

Upton, J., Cole, P. D., Shaw, P., Szakacs, A., and Seghedi, I. (2002). "Correlation of tephra layers found in southern Romania with the Campanian Ignimbrite (~37 ka)," in The Quaternary Research Association and First Postgraduate Paleo-environmental Symposium (Amsterdam: Universiteit van Amsterdam), 36.

Veres, D., Lane, C. S., Timar-Gabor, A., Hambach, U., Constantin, D., Szakács, A., et al. (2013).

1218 The Campanian Ignimbrite/Y5 tephra layer - A regional stratigraphic marker for Isotope Stage 3
1219 deposits in the Lower Danube region, Romania. ***Quat. Int.*** 293, 22–33.
1220 doi:10.1016/j.quaint.2012.02.042

1221 Vitale, S., and Isaia, R. (2014). Fractures and faults in volcanic rocks (Campi Flegrei, southern Italy):
1222 insight into volcano-tectonic processes. ***Int. J. Earth Sci.*** 103, 801–819. doi:10.1007/s00531-
1223 013-0979-0

1224 Walker, G. P. L. (1972). Crystal Concentration in Ignimbrites. ***Contrib. Mineral. Petrol.*** 36, 135–
1225 146. doi:10.1007/BF00371184

1226 Walker, G.P.L. (1973). Explosive volcanic eruptions — a new classification scheme. ***Geol. Rundsch.***
1227 62, 431–446. doi:10.1007/BF01840108

1228 Walker, G. P. L. (1980). The Taupo pumice: Product of the most powerful known (ultraplinian)
1229 eruption? ***J. Volcanol. Geotherm. Res.*** 8, 69–94. doi:10.1016/0377-0273(80)90008-6

1230 Walker, G. P. L. (1983). Ignimbrite types and ignimbrite problems. ***J. Volcanol. Geotherm. Res.*** 17,
1231 65–88. doi:10.1016/0377-0273(83)90062-8

1232 Walker, G. P. L., and Croasdale, R. (1970). Two Plinian-type eruptions in the Azores. ***J. Geolog. Soc.***
1233 127, 17–55. doi:10.1144/gsjgs.127.1.0017

1234 Wilson, C. J. N. (1991). Ignimbrite morphology and the effects of erosion: a New Zealand case
1235 study. ***Bull. Volcanol.*** 53, 635-644. doi:10.1007/BF00493690

1236 Wilson, C. J. N. (2001). The 26.5 ka Oruanui eruption, New Zealand: an introduction and overview.
1237 ***J. Volcanol. Geotherm. Res.*** 112, 133-174. doi:10.1016/S0377-0273(01)00239-6

1238 Wilson, C. J. N., and Walker, G. P. L. (1985). The Taupo eruption, New Zealand. 1. General aspects.
1239 ***Philos. Trans. R. Soc. A Math. Phys. Eng. Sci.*** 314, 199–228. doi:10.1098/rsta.1985.0019

1240 Wood, R. E., Douka, K., Boscato, P., Haesaerts, P., Sinitsyn, A., and Higham, T. (2012). Testing the
1241 ABOx-SC method: dating known-age charcoals associated with the Campanian Ignimbrite.
1242 ***Quat. Geochronol.*** 9, 16-26. doi:10.1016/j.quageo.2012.02.003

1243 Woods, A. W., and Wohletz, K. (1991). Dimensions and dynamics of co-ignimbrite eruption
1244 columns. ***Nature***, 350, 225-227. doi:10.1038/350225a0

1245 Wulf, S., Kraml, M., Brauer, A., Keller, J., and Negendank, J. F. W. (2004). Tephrochronology of the
1246 100 ka lacustrine sediment record of Lago Grande di Monticchio (southern Italy). ***Quat. Int.***
1247 122, 7–30. doi:10.1016/j.quaint.2004.01.028

1248 Yang, Q., and Bursik, M. (2016). A new interpolation method to model thickness, isopachs, extent,
1249 and volume of tephra fall deposits. ***Bull. Volcanol.*** 78. 68–21. doi:10.1007/s00445-016-1061-0

1250 Yokoyama, S. (1974). Mode of movement and emplacement of Ito pyroclastic flow from Aira
1251 caldera, Japan. Science Reports, Tokyo Kyoiku Daigaku 12, 17-62.

1252 Yokoyama, S. (1985). Geomorphological aspects of large-scale pyroclastic flow deposits: a review.
1253 Transactions, Japanese Geomorphological Union 6, 131-152.

Zanchetta, G., Giaccio, B., Bini, M., and Sarti, L. (2018). Tephrostratigraphy of Grotta del Cavallo, Southern Italy: Insights on the chronology of Middle to Upper Palaeolithic transition in the Mediterranean. *Quat. Sci. Rev.* 182, 65-77. doi:10.1016/j.quascirev.2017.12.014

10 Data Availability Statement

The datasets generated and analyzed for this study can be found in the Data Repository https://mfr.osf.io/render?url=https%3A%2F%2Fosf.io%2Fc8nea%2Fdownload. QGIS data are available on request to the corresponding author.